
Are we Done with Object Recognition? The iCub robot’s Perspective.

Giulia Pasquale · Carlo Ciliberto · Francesca Odone · Lorenzo Rosasco ·
Lorenzo Natale

Abstract We report on an extensive study of the current benefits and limitations of deep learning approaches to robot vision and introduce a novel dataset used for our investigation. To avoid the biases in currently available datasets, we consider a human-robot interaction setting to design a data-acquisition protocol for visual object recognition on the iCub humanoid robot. Considering the performance of off-the-shelf models trained on off-line large-scale image retrieval datasets, we show the necessity for knowledge transfer. Indeed, we analyze different ways in which this last step can be done, and identify the major bottlenecks in robotics scenarios. By studying both object categorization and identification tasks, we highlight the key differences between object recognition in robotics and in image retrieval tasks, for which the considered deep learning approaches have been originally designed. In a nutshell, our results confirm also in the considered setting the remarkable improvements yield by deep learning, while pointing to specific open challenges that need to be addressed for seamless deployment in robotics.

Keywords Humanoid Robotics · iCub · Machine Learning · Deep Learning · Object Recognition · Transfer Learning · Dataset · Invariance

G. Pasquale · C. Ciliberto · L. Rosasco · L. Natale
iCub Facility,
Laboratory for Computational and Statistical Learning,
Istituto Italiano di Tecnologia
Via Morego 30, 16163, Genova, IT
E-mail: giulia.pasquale@iit.it

G. Pasquale · F. Odone · L. Rosasco
Dipartimento di Informatica, Bioingegneria, Robotica e Ingegneria dei Sistemi, Università degli Studi di Genova
Via Dodecaneso 35, 16100, Genova, IT

1 Introduction

Artificial intelligence has recently progressed dramatically, largely thanks to the advance in deep learning. Computational vision, specifically object classification, is perhaps the most obvious example where deep learning has achieved so stunning results to raise the question of whether this problem is actually solved (Krizhevsky et al 2012b; Simonyan and Zisserman 2015; Szegedy et al 2015; He et al 2016). Should this be the case, robotics would be a main field where the benefits could have far reaching effect. Indeed, the lack of reliable visual skills is largely considered a main bottleneck for the successful deployment of robotics systems in everyday life (Kemp et al 2007).

With this perspective in mind, we have recently started an effort to isolate and quantify the benefits and limitations, if any, of deep learning approaches to object recognition in robotics (Pasquale et al 2015, 2016a). Clearly, visual perception is only one of the possible sensory modalities enabling object recognition in robotics (Montesano et al 2008; Chitta et al 2011; Dahiya et al 2010; Natale et al 2004; Gorges et al 2010; Sinapov et al 2014a; Hosoda and Iwase 2010; Moldovan et al 2012) and indeed, the comparison with human intelligence suggests there is more than “just” vision to object recognition (Metta et al 2006; Fitzpatrick et al 2008; Pinto et al 2016). Nonetheless, current deep learning based artificial vision systems perform so well, that it seems natural to ask how far they can go, before further perceptual cues/modalities are needed. To this end, in this work we mainly focus on object recognition tasks in robotics using only visual cues.

To investigate the effectiveness of deep learning approaches in robotic applications, we designed a dataset tailored to reflect a prototypical visual “experience” of a humanoid robot. Indeed, the remarkable performance of deep learning methods in object recognition has been

primarily reported on computer vision benchmarks such as (Griffin et al 2007; Everingham et al 2010, 2015; Russakovsky et al 2015), which have been essentially designed for image retrieval tasks, and hardly are representative of a robotics scenario. In fact, this is a motivation common to other recent works such as (Lai et al 2011; Oberlin et al 2015; Borji et al 2016), where new datasets have been proposed.

Using the iCub robot (Metta et al 2010), we devised a human-robot interaction framework to acquire a corresponding dataset, named iCWT (iCubWorld Transformations). This dataset is rich and easy to expand to include more data and complex perceptual scenarios. It includes several object categories with many instances per category, hence allowing to test both categorization and identification capabilities. Notably, the dataset is segmented in different sets of views, with the purpose of testing specifically robustness and invariance properties of recognition systems within a realistic robotic scenario.

Provided with the iCWT dataset, we performed extensive empirical investigation using different state of the art Convolutional Neural Networks (CNN) architectures (Krizhevsky et al 2012a; Simonyan and Zisserman 2015; Szegedy et al 2015; He et al 2016). We began checking to which extent systems already trained (on other data) could be directly tested on iCWT. While obtaining results much better than chance, these systems do not perform accurately enough in this case - as perhaps one could expect. We hence followed a recent trend based on the general idea of transfer learning (Schwarz et al 2015; Oquab et al 2014; Sünderhauf et al 2015; Pasquale et al 2016b; Chatfield et al 2014; Simonyan and Zisserman 2015), where the pretrained networks are adapted (fine-tuned) to the data at hand. Indeed, our results confirm the effectiveness of these strategies obtaining substantial improvements.

While impressive, these methods did not quite provide the close to perfect accuracy one would wish for. We hence proceeded taking a closer look at the results, starting from the question of whether the missing gap could be imputed to lack of data. Indeed, CNNs are known to need massive amount of data to work and data-augmentation is often used to improve results. As we discuss in detail later in the paper, investigating this latter question highlighted some differences between iCWT and other datasets such as ImageNet (Russakovsky et al 2015). More generally, we identified clear differences between the object recognition task in robotics with respect to scenarios typically considered in learning and vision.

Along the way, our analysis allowed to test invariance properties of the considered deep learning net-

works and quantify their merits not only for categorization but also for identification. The description and discussion of our empirical findings is concluded with a critical review of some of the main venue of improvements, from a pure machine learning perspective but also taking extensive advantage of the robotic platform. Indeed, bridging the gap in performance appears to be an exciting avenue for future multidisciplinary research.

In the next subsection we discuss several related works, while the rest of the paper is organized as follows: Sec. 2 introduces the iCWT dataset and its acquisition setting. In Sec. 3 we review the deep learning methods considered for our empirical analysis, which is reported in Sec. 4 for the categorization task and in Sec. 5 for object identification. Sec. 6 concludes our study with the review of possible directions of improvement for visual recognition in robotics.

1.1 Deep Learning for Robotics

Deep Learning methods are receiving growing attention in robotics, and are being adopted for a variety of problems such as object recognition (Schwarz et al 2015; Pinto et al 2016; Held et al 2016; Pasquale et al 2016a), place recognition and mapping (Sünderhauf et al 2016, 2015), object affordances (Nguyen et al 2016), grasping (Redmon and Angelova 2014; Pinto and Gupta 2015; Levine et al 2016) and tactile perception (Baishya and Bäuml 2016). We limit our discussion to the work on object recognition, which is more relevant to the work described in this paper.

In (Schwarz et al 2015) the authors demonstrate transfer learning from pre-trained deep Convolutional Neural Networks (CNNs) and propose a way to include depth information from an RGB-D camera. The main idea is to extract a feature vector from the CNN and train a cascade of Support Vector Machines (SVMs) to discriminate objects' class, identity and position. Depth data is encoded in a planar image using a colorization scheme. The authors report performance increase on the Washington RGB-D benchmark (Lai et al 2011). The work in (Pinto et al 2016) shows how the robot can use self-generated explorative actions (like pushing and poking objects) to autonomously extract training data and train a CNN.

In this paper we employ a less constrained setting than (Schwarz et al 2015), in that CNNs are trained with data acquired by the robot during natural interaction (which undergo therefore more challenging view-point transformations). We employ similar techniques for transfer learning, but we consider a wider range of architectures and fine tuning techniques. In contrast to (Pinto et al 2016) the use of a human teacher (see

Sec. 2 for details on the acquisition setup) gives us more control on the object transformations. Clearly, our work could be extended by introducing self-supervision using explorative actions similar to the ones in (Pinto et al 2016).

The work in (Held et al 2016) and our work in (Pasquale et al 2016a) are similar to the work presented in this paper in that they investigate invariance properties of CNNs and learning from few examples. They focus, however, on instance recognition, whereas in this paper we consider – thus significantly extending (Pasquale et al 2016a) – the problem of object categorization. In addition we perform a detailed investigation of various fine-tuning techniques and systematic evaluation of the recognition performance for specific object transformations.

1.2 Datasets for Visual Recognition in Robotics

In the literature, several datasets for visual recognition in robotics have been proposed: COIL (Nene et al 1996), ALOI (Geusebroek et al 2005), Washington RGB-D (Lai et al 2011), KIT (Kasper et al 2012), SHORT-100 (Rivera-Rubio et al 2014), BigBIRD (Singh et al 2014), Rutgers Amazon Picking Challenge RGB-D Dataset (Renzie et al 2016). One of the main characteristic of these datasets is to capture images of an object while it undergoes specific viewpoint transformations. However, these datasets are usually acquired in strictly controlled “turntable” settings, aiming to provide accurate 3D annotations (e.g., information about the object’s pose in each image) as a ground truth for grasping or manipulation, rather than substantial variations in the objects’ appearance. As a consequence, they mainly contain changes in the 3D point of view, under-representing other visual transformations, such as scaling, background changes and so forth, which are fundamental to benchmark visual recognition tasks. For instance, (Bakry et al 2015) use the Washington RGB-D and the Pascal 3D+ (Xiang et al 2014) datasets in order to evaluate the invariance of deep learning methods, and their analysis consequently focuses mainly to 3D viewpoint changes. Moreover, since the object is typically positioned on a turntable that is subsequently rotated, these dataset do not show more natural object transformations that often occur in practice. See (Leitner et al 2015) for a review of the major limitations of current datasets.

The NORB dataset (LeCun et al 2004) was also acquired in a similar turntable setting, but it is one of the first to be released specifically in support of the investigation of invariance properties of recognition methods, and in fact the images in the dataset have been artificially perturbed in order to increase variability. Re-

cently, (Borji et al 2016), motivated by similar considerations, presented the iLab-20M dataset: specifically, the authors aim to create a large-scale visual recognition benchmark which, beyond representing a high number of object instances, provides also a sufficient number of images per object, in order to study invariance properties of deep learning methods. Also iLab-20M is acquired in a turntable setting, in order to collect annotations for each image in terms of the object’s pose.

The iCWT dataset presented in this paper separates from most previous work in that objects are captured while undergoing “natural” transformations. Acquisition is performed in a “semi-controlled” setting intended to be a benchmark reproducing typical uncertainties faced by the visual recognition system of a robot during a real-world task. In the following, we discuss the iCWT dataset and the related acquisition setting in detail.

2 The iCubWorld Dataset

In this section we present a novel dataset for visual recognition, iCubWorld Transformations (iCWT), which is used for the empirical analysis in this work. iCWT is the latest release of the iCubWorld¹ project, whose goal is to benchmark and improve visual recognition systems for robotics. iCubWorld datasets (Ciliberto et al 2013; Fanello et al 2013b; Pasquale et al 2015) are designed to record a prototypical visual “experience” of a robot, the humanoid iCub (Metta et al 2010), while it is performing vision-based tasks. To this end, we devised and implemented a simple human-robot interaction application, during which we directly acquire images for the dataset from the robot’s cameras.

There is a remarkable advantage in collecting iCubWorld directly from the robot platform. Indeed, the resulting dataset offers a natural testbed for visual recognition in robotics, which is as close as possible to the real application. In particular, this ensures that performance measured *off-line* on iCubWorld can be expected to generalize well when the system is deployed on the actual robot. Note that this aspect of iCubWorld is extremely relevant since visual biases make it typically difficult to generalize prediction performances across different datasets and applications, as already well-known from previous work (Pinto et al 2008; Torralba and Efros 2011; Khosla et al 2012; Hoffman et al 2013; Rodner et al 2013; Model and Shamir 2015; Stamos et al 2015; Tommasi et al 2015) and shown empirically in Sec. 4.1 of this paper.

¹ <https://robotology.github.io/iCubWorld/>

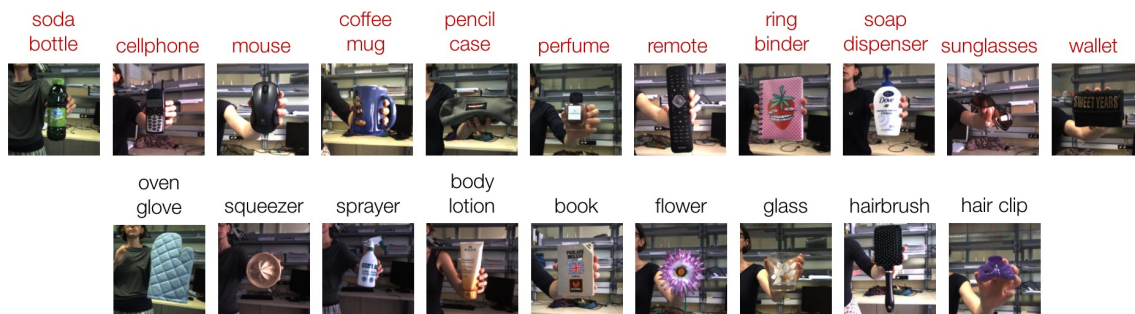


Fig. 1 iCWT categories. For each category in iCWT, we report one example image for one instance. (Red) categories appear also in the ILSVRC 2012 dataset. (Black) categories appear in ImageNet but not in ILSVRC (see supplementary material for more details).

Currently, to acquire iCubWorld releases we did not make extensive use of the robot’s physical capabilities (e.g., manipulation, exploration, etc.). This was done because current deep learning methods achieve already remarkable performance by relying solely on visual cues and our goal was to evaluate their accuracy in *isolation* on in a robotic setting. Indeed, while exploiting the robot body could provide further dramatic advantages to modeling and recognition (see for instance (Montesano et al 2008) and, more recently, (Moldovan et al 2012), (Leitner et al 2014) and (Dansereau et al 2016)), it would also prevent us to correctly assess the contribution of the purely visual components.

2.1 Acquisition Setup

Data acquisition for iCWT followed a protocol similar to the one in (Fanello et al 2013a), which was adopted for previous iCubWorld releases (Ciliberto et al 2013; Fanello et al 2013b; Pasquale et al 2015): a human “teacher” shows an object to the robot and pronounces the associated label to annotate subsequent images. The robot exploits bottom-up visual cues to track and collect images of the object while the human actor moves it and shows it from different poses. In this work we decided to adopt an object tracker using depth information (Pasquale et al 2016b), in place of one exploiting the detection of independent motion in the scene (Ciliberto et al 2011, 2012) (which has been used to collect previous iCubWorld releases). In fact, as shown in (Pasquale et al 2016b), this allows us to extract a more precise bounding box around the object of interest.

We developed an application to scale this acquisition procedure to hundreds of objects, which were collected during multiple interactive sessions. iCWT is available on-line and we plan to make also this application publicly available in order for other laboratories to use the same protocol to collect their own (or

possibly contribute to) iCubWorld. Indeed, there are few datasets for visual recognition in the literature that were acquired directly on a robotic platform (Ramisa et al 2011; Meger and Little 2013; Oberlin et al 2015). One common reason is that scaling up the dataset size is extremely expensive and time consuming when using a single robot. To this end, an appealing solution, proposed in the Million Object Challenge project (Oberlin et al 2015), is to involve multiple robots to collect a shared dataset of visual experiences.

Note that, while we used an initial subset of iCWT in (Pasquale et al 2016a), in this paper we present the dataset for the first time in its entirety.

2.2 Dataset Overview

iCWT is the largest iCubWorld release so far, comprising 200 objects evenly organized into 20 categories that can be typically found in a domestic environment. Fig. 1 reports a sample image for each category in iCWT: 11 categories (in red in the figure) are also in the ImageNet Large-Scale Visual Recognition Challenge (ILSVRC) 2012 (Russakovsky et al 2015), i.e. we found semantically and visually similar classes among the 1000 of the classification challenge. The remaining 9 categories do not appear ILSVRC but belong (or are similar) to a synset in the larger ImageNet dataset (Deng et al 2009). To provide a qualitative intuition of the semantic variability within a given category, namely the different visual appearance of objects in the same category, Fig. 2 shows a sample image from the 10 instances in the *mug* category. We refer the reader to the supplementary material (Fig. 13) for example images of all object instances in iCWT.

The peculiarity of iCWT, motivating its name, is that each object is shown in multiple image sequences while it undergoes specific visual transformations (such as rotations, scaling or background changes). This is done to test the invariance of visual models in robotics.



Fig. 2 Semantic variability. Sample images for the different object instances in the *mug* category to provide a qualitative intuition of the semantic variability in iCubWorld. See Fig. 13 in the supplementary material for more examples.

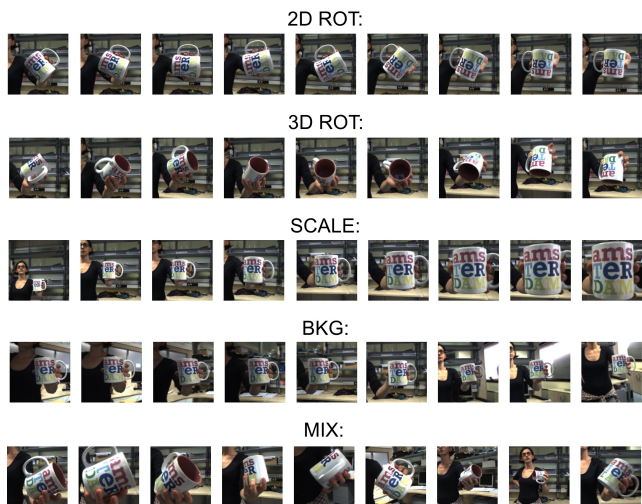


Fig. 3 Visual transformations. Excerpts from the sequences acquired for one mug, representing the object while it undergoes specific visual transformations.

Indeed, since very few works study “real” (i.e. non-synthetic) visual transformations (Goodfellow et al 2009) in order to evaluate the invariance properties of visual representations, we believe that iCWT could be a significant contribution in this direction. To our knowledge, iCWT is the first dataset to address invariance-related questions in robotics and accounts a much wider range of visual transformations with respect to previous datasets.

For each object instance, we acquired 5 different image sequences, each while the human supervisor performed a different visual transformation to the object. Fig. 3 reports excerpts of these sequences, that contain, respectively:

2D Rotation The human rotated the object parallel to the camera image plane. The same scale and position of the object were maintained (see Fig. 3, first row).

3D Rotation Similarly to 2D rotations, the object was kept at same position and scale. However, this time the human applied a generic rotation to the object (not parallel to the image plane). As a consequence different “faces” of the object were shown to the camera (Fig. 3, second row).

Scale The human moved the object towards the camera and back, thus changing the object’s scale in

Table 1 Summary of the *iCubWorld - Transformations* dataset

# Categories	# Obj. per Category	# Days	Transformations	# Frames per Session
20	10	2	2D ROT, 3D ROT SCALE, BKG MIX	150 300

the image. No change in the object orientation (no 2D or 3D rotation) was applied (Fig. 3, third row).

Background The human moved the object around the robot, keeping approximately the same distance (scale) and pose of the object with respect to the camera plane. During this acquisition process only the background changes while the object appearance remains approximately the same (Fig. 3, fourth row).

Mix The human moved the object freely in front of the robot, as a person would naturally do when showing a new item to a child. In this sequence all nuisances in all combinations can appear (Fig. 3, fifth row).

Each sequence is composed by approximately 150 images acquired at 8 frames per second in the time interval of 20s, except for the *Mix* one that lasted 40s and comprises ~ 300 images. As anticipated, the acquisition of the 200 objects was split in multiple sessions performed in different days. The acquisition location was always the same (with little uncontrolled changes in the background across days). The lighting condition was not artificially controlled, since we wanted to investigate its role as a further nuisance: to this end, we acquired objects at different times of the day and in different days, so that lighting conditions are slightly changing across the 200 objects (but not within the five sequences of an object, which were all acquired in the span of few minutes). Moreover, we repeated the acquisition of each object in two different days, so that we ended up with 10 sequences per object, containing 5 visual transformations in 2 different light conditions. The adopted iCub’s cameras resolution is 640×480 . We recorded the centroid and bounding box provided by the tracker at each frame (for details about this procedure see (Pasquale et al 2016b)). Both left and right images were acquired, to allow for offline computation of the disparity map and potentially further improvement of the object’s localization and segmentation. Tab. 1 summarizes the main characteristics of iCubWorld-Transformations.

3 Methods

In this section we review the learning methods considered in this work. In particular we briefly introduce the principal concepts behind deep Convolutional Neural

Networks (CNNs), describe the architectures used in our analysis and the algorithms adopted to train and apply them. We refer the interested reader to (Goodfellow et al 2016) for an in-depth introduction to CNNs and deep learning in general.

3.1 Deep Convolutional Neural Networks

Deep Convolutional Neural Networks (CNNs) are hierarchical models organized as the concatenation of multiple processing layers. This structure allows mapping the input signal (such as images, speech, etc.) through a series of subsequent *representations* to progressively select the features that are most relevant to the considered task. The prototypical structure of a CNN (see Fig. 4) performs at each layer (usually referred to as *convolution* layer) the following set of operations:

- **Convolutions:** local convolution with respect to a bank of (learned) linear filters.
- **Spatial Downsampling** for instance using strided convolutions.
- **Element-wise Non Linearity** such as sigmoid functions (Bishop 2006) or, more recently Rectifying Linear Units (He et al 2015).
- **Spatial Pooling** to aggregate local responses to the signal in a single component, for instance by taking the maximum value observed (max-pooling).

Each CNN architecture is characterized by the specific choice and implementation of the operations above. The filters, locally processing the input signal at each layer, are typically learned by minimizing a desired loss function, such as the overall classification accuracy in supervised settings or the reconstruction error in unsupervised ones. The spatial downsampling and pooling operations make the representation more robust to transformations of the input at increasingly larger scales. The non-linearities selectively retain only features that are relevant to the task, while suppressing the others.

Until recently, the most common strategy in image classification settings was to follow convolution layers (C) with a set of *fully connected* layers (FC), namely a standard multi-layer Neural Network. In the last few years however, architectures with fewer or even just one FC layer have started to be preferred since they achieve comparable or better performance while optimizing significantly fewer parameters (Szegedy et al 2015; He et al 2016). In classification settings, the final layer of a network is typically a *softmax* function that maps the CNN output into individual class likelihood scores. The CNN

prediction is then obtained by choosing the class with maximum score.

The modular structure of CNNs allows training their parameters simultaneously for all layers (also known as *end-to-end learning*) via back-propagation (LeCun et al 1989). Given the large number of parameters to be optimized (in the order of millions), CNNs typically need large amounts of training data to achieve good performance. Various forms of data augmentation are often needed to artificially increase the number of training examples (e.g. by synthetically modifying the images via geometrical or illumination changes). To further mitigate the risk of overfitting, regularization techniques such as weights L2 regularization, dropout (Hinton et al 2012; Srivastava et al 2014) or, more recently, batch normalization (Ioffe and Szegedy 2015), have proved helpful.

In this work we investigate the performance of modern CNNs on the robotic setting of iCubWorld. For this analysis we selected recent architectures achieving the highest accuracy on the ImageNet Large-Scale Visual Recognition Challenge (ILSVRC) (Russakovsky et al 2015) between 2012 and 2015. We used their corresponding implementation trained on ILSVRC 2012 and publicly available within the CAFFE (Jia et al 2014) framework. Below we summarize their structures:

CaffeNet⁴ A small variation of the AlexNet model, winner of ILSVRC 2012 (Krizhevsky et al 2012a). Concatenates 5C + 3FC layers comprising $\sim 60M$ parameters.

VGG-16⁵ Second classified at ILSVRC 2014 (Simonyan and Zisserman 2015). It maintains the general structure of AlexNet (but with 13C + 3FC layers comprising $\sim 140M$ parameters). It is relatively expensive to train in terms of memory and time because of the large FC layers.

GoogLeNet⁶ Winner of ILSVRC 2014 (Szegedy et al 2015). It diverges from previous architectures in that it concatenates so called *inception modules* and uses just one FC layer at the very end, reducing the parameters number to $\sim 4M$ for 22 layers.

ResNet-50⁷ The name is short for *residual networks*, which won the ILSVRC 2015 (He et al 2016), of which ResNet-50 is a smaller version stacking 50 layers in $\sim 20M$ parameters.

⁴ https://github.com/BVLC/caffe/tree/master/models/bvlc_reference_caffenet

⁵ [http://www.robots.ox.ac.uk/\\$\sim\\$sim\\$vgg/research/very_deep/](http://www.robots.ox.ac.uk/\simsim$vgg/research/very_deep/)

⁶ https://github.com/BVLC/caffe/tree/master/models/bvlc_googlenet

⁷ <https://github.com/KaimingHe/deep-residual-networks>

³ <https://www.clarifai.com/technology>

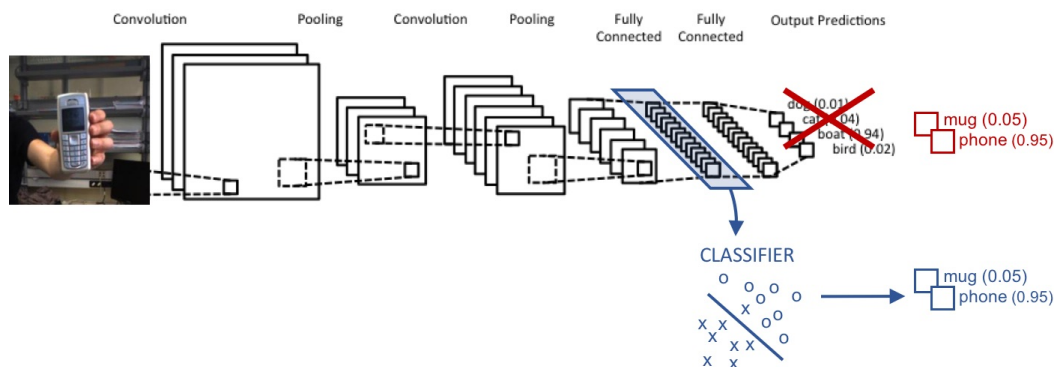


Fig. 4 Example of a Convolutional Neural Network (Sec. 3.1) and of the two knowledge transfer approaches considered in this work (Sec. 3.2). **(Blue pipeline) feature extraction:** in this case the response of one of the layers is used as a feature vector for a “shallow” predictor like RLSCs, SVMs (see Sec. 3.2.1), which is trained on the new task. **(Red pipeline) fine-tuning:** in this case the network is trained end-to-end to the new task by replacing the final layer and using the original model as a “warm-restart” (see Sec. 3.2.2). Network image from³.

3.2 Transfer Learning Techniques

Deep learning methods typically require very large datasets to be successfully trained. While this could in principle prevent their applicability to problems where training data is scarce, recent empirical evidence has shown that knowledge acquired by training a network on a large-scale problem can be “transferred” to the new domain. Different approaches to implement this strategy have been proposed in the literature. In this section we review two of the most well-established method, which we empirically assess in our experiments, namely *feature extraction* and *fine-tuning*.

3.2.1 Feature Extraction

It has been observed that deeper layers of a CNN selectively respond to specific properties of the visual scene that are typically characteristic of specific objects or object parts. (Chatfield et al 2014; Yosinski et al 2014; Donahue et al 2014; Zeiler and Fergus 2014). These responses can be interpreted as representations of the visual input responding only to features that are most relevant to the task at hand. Following this intuition, it has been shown that CNNs trained on large-scale datasets can be indeed used as “feature extractors” on smaller datasets, leading to remarkable performance (Schwarz et al 2015; Oquab et al 2014; Sünderhauf et al 2015; Pasquale et al 2016b). This is typically done by training a standard classifier such as a Support Vector Machine (SVM) or a Regularized Least Squares Classifier (RLSC) (Bishop 2006) on top of feature vectors obtained from one or multiple layer responses. This strategy, depicted in Fig. 4 (Blue pipeline), can be interpreted as changing the last layer of the CNN and train-

ing it on the new dataset while keeping all other parameters of the network fixed.

Implementation Details. In the empirical analysis of this work we used feature extraction as a strategy to transfer knowledge from CNNs trained on ImageNet to iCWT. The specific layers used for our experiments are reported in Tab. 2 for the four architectures considered in this paper. We used RLSC with a Gaussian Kernel as classifier for the CNN-extracted features. In particular we implemented the Nystrom sub-sampling approach considered in (Rudi et al 2015, 2016), which is computationally appealing for mid and large-scale settings and indeed allowed to significantly speed up our experimental evaluation. We refer the reader to the supplementary material for details about the model selection and image preprocessing protocols adopted in this work.

3.2.2 Fine-tuning

A CNN trained on a large-scale dataset can be used to “warm-start” the learning process on other (potentially smaller) domains. This strategy, known as *fine-tuning* (Chatfield et al 2014; Simonyan and Zisserman 2015), consists in performing back-propagation on the new training set by initializing the parameters of the network to those previously learned (see Fig. 4 (Red pipeline)). In these settings it is necessary to adapt the final layer to the new task (e.g. by changing the number of units in order to account to the new number of classes to discriminate).

A potential advantage of fine-tuning is that it adapts the parameters of all networks’ layers to the new problem rather than only those in the final layers. How-

Table 2 Feature extraction layers for the four architectures considered in this work. We used the notation adopted in the literature, in which the number identifies the layer number and the label specifies its type (i.e. fully connected or pooling layer).

Model	Output Layer
CaffeNet	fc6 or fc7
GoogLeNet	pool5/7x7_s1
VGG-16	fc6 or fc7
ResNet-50	pool5

Table 3 Fine-tuning protocols for *CaffeNet* and *GoogLeNet*. Base LR is the starting learning rate of all layers that are initialized with the original model. The FC layers that are learned from scratch are indicated using their names in CAFFE models (2^{nd} row), specifying the starting learning rate used for each of them. For the other parameters, we refer the reader to CAFFE documentation.

	CaffeNet		GoogLeNet	
	<i>adaptive</i>	<i>conservative</i>	<i>adaptive</i>	<i>conservative</i>
Base LR	1e-3	0	1e-5	0
Learned FC Layers	fc8: 1e-2	fc8: 1e-4 fc7: 1e-4 fc6: 1e-4	loss3/classifier: 1e-2 loss1(2)/classifier: 1e-3 loss1(2)/fc: 1e-3	
Dropout (%)		fc7: 50 fc6: 50	pool5/drop_7x7_s1: 60 loss1(2)/drop_fc: 80	
Solver		SGD	Adam	
LR Decay Policy		Polynomial (exp 0.5)	No decay	
# Epochs	6	36	6	
Batch Size		256	32	

ever, this flexibility comes at the price of a more involved training process. Indeed, the performance of a fine-tuned network are extremely dependent on the choice of the (many) hyper-parameters available. Fine-tuning has been recently used to adapt network models learned on ImageNet to robotic tasks (see, e.g., (Eitel et al 2015; Pinto and Gupta 2016; Redmon and Angelova 2015a; Pasquale et al 2016a; Nguyen et al 2016)).

Implementation Details. In our experiments we performed fine-tuning only for *CaffeNet* and *GoogLeNet*, which are representative of most recent architectures and were significantly faster to fine-tune than *VGG-16* and *ResNet-50*. We considered two main regimes for fine-tuning a network: one updating only one or more FC layers while keeping the others fixed, and another one more aggressively adapting all layers, comprising the C layers, to the training dataset. This was done by selecting different learning rates for the neurons in each layer, i.e., the size of gradient steps at each iteration of back-propagation. We refer to these two protocols as *conservative* and *adaptive* and report the corresponding parameters in Tab. 3 as a reference. In the experiments discussed in this paper we consider only these strategies since we did not observe significant performance differences following other choices of parameters. We

refer to the supplementary material of this work for an analysis of using other fine-tuning parameters and a discussion on the model selection protocols used in our experiments.

4 Results (Categorization)

In this section we present our empirical investigation of Deep Learning methods in the robotic setting of iCubWorld.

4.1 Deep Learning and (the Need for) Knowledge Transfer

Modern datasets for visual recognition comprise an extremely large number of images (e.g. 1 Million for the ILSVRC challenge) depicting objects in a wide range of natural scenes. This extreme variability opens the question of whether datasets such as iCubWorld, which represent a smaller “reality”, could be interpreted simply as sub-domains of larger ones. If this was the case, deep learning models trained on ImageNet would achieve high recognition performance on iCubWorld as well, without any re-training or adaptation.

While this result would lead to the appealing scenario where a robot can simply download and use a visual classifier “off-the-shelf” (i.e. trained off-line), previous analysis has shown that most computer vision datasets are essentially biased, ultimately preventing a learning algorithm to generalize from one domain to the other (Pinto et al 2008; Torralba and Efros 2011; Model and Shamir 2015; Khosla et al 2012; Stamos et al 2015; Tommasi et al 2015; Hoffman et al 2013; Rodner et al 2013). Similarly, it was recently observed that conventional “non-deep” models trained on ImageNet perform poorly when applied to robotic settings (Goehring et al 2014).

To address this question, we evaluated four off-the-shelf CNNs (the ones reviewed in Sec. 3.1) for the task of image classification on iCWT. For these experiments we restricted the test set to the 11 categories of iCWT that appear also in the ILSVRC challenge (see Sec. 2 and Fig. 1). As a reference, we compared these results with the average accuracy of the same networks on the corresponding 11 categories of the ImageNet dataset. The test set for iCWT was composed, for each category, by the images of all 10 object instances, comprising all 5 transformations for one day and the left camera (unless differently specified we always used this camera for the experiments), for a total of ~ 9000 images per category. For ImageNet, we downloaded the images for the corresponding 11 categories (refer to the supplementary

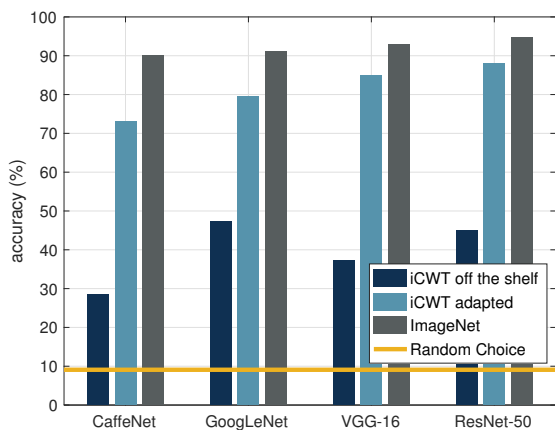


Fig. 5 Average classification accuracy of off-the-shelf networks (trained on ILSVRC) tested on iCubWorld (Dark Blue) or on ImageNet itself (Gray). The test sets for the two datasets are restricted to the 11 shared categories (see Sec. 2). (Light Blue) reports the classification accuracy when the same networks are “transferred” to iCubWorld (see Sec. 4.1 for details). The (Orange line) shows the recognition chance of a random classifier.

material for the corresponding synsets), comprising on average ~ 1300 images per category.

Fig. 5 reports the average classification accuracy on iCWT (Dark Blue) and ImageNet (Gray). It can be immediately observed that there is a substantial drop in performance of $\sim 50 - 60\%$ when testing on iCWT rather than ImageNet, suggesting that differences between the two datasets exist, and in particular that iCubWorld is not a sub-domain of ImageNet. This drop is likely due to biases in ImageNet (see also (Tommasi et al 2015; Hoffman et al 2013; Rodner et al 2013)). While an in-depth analysis of bias is outside the scope of this work, in the supplementary material we provide some further evidence of this effect. We care to point out that for a fair comparison we have restricted the output of the off-the-shelf networks to the 11 classes considered in the experiment with iCWT (from the original 1000-dimensional output vector provided by the off-the-shelf networks). We refer again to the supplementary material for the experiments reporting the same performance when considering the entire 1000-dimensional prediction.

Knowledge Transfer. The drop in performance observed in Fig. 5 implies that it is necessary to train the recognition system on the target domain. However, the experiment also shows that all the networks performed substantially better than chance (Orange line). This suggests that the networks retained some knowledge about the objects’ appearance. Therefore, rather than training a novel architecture “from scratch” (which typ-

ically requires large amounts of training data, time and computational resources), a viable alternative is to transfer such knowledge, essentially by “adapting” the networks trained on ImageNet to the new setting (see Sec. 3.2). The idea of knowledge transfer has recently received considerable attention from the Deep Learning community (Hoffman et al 2013; Agrawal et al 2014; Azizpour et al 2015; Huh et al 2016) because it provides a robust approach to apply Deep Learning methods to smaller datasets.

In Fig. 5 we report the classification performance achieved by systems where knowledge transfer has been applied (Light Blue). For these experiments we followed the protocol described in Sec. 3.2.1, where RLSC predictors are trained on feature vectors extracted from the deeper layers of the CNNs. We created a separate training set from iCWT, by choosing 9 instances for each category for training while keeping the 10th instance for testing. We repeated these experiments for 10 trials in order to allow each instance of a category to be used in the test set. Fig. 5 reports the average accuracy over these trials. We observe a sharp improvement for all networks, which achieve a remarkable classification accuracy in the range of $\sim 70 - 90\%$. On ImageNet however, the corresponding performance is still significantly higher, although such gap seems to be reduced for more recent architectures.

What are the reasons for this gap? In the following we empirically address this question, showing that the observed behavior is due to fundamental differences between robot vision and image retrieval settings.

4.2 Do we need more data?

Deep learning methods require large amounts of data in order to be trained effectively. This is particularly true when training a network from “scratch”, but valid also (albeit on a smaller scale) to knowledge transfer techniques. Indeed, as mentioned in Sec. 3, a common practice when training a CNN is to perform *data augmentation*, namely to artificially increase the dataset size by applying synthetic transformations to the original images (e.g. rotations, reflections, crops, illumination changes, etc.).

From this perspective the robotic setting seems particularly favorable. Indeed, data augmentation can be performed by simply acquiring more and more *frames* depicting an object while viewpoint or illumination change naturally. While acquiring more frames of an object is particularly convenient, in robotics it is typically expensive to gather instead images depicting different objects *instances*, since the robot needs to directly observe each of them. In this section we investigate the impact

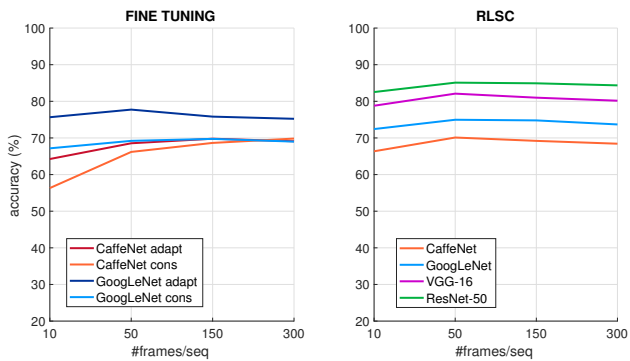


Fig. 6 Recognition accuracy vs # frames. (Left) Accuracy of *CaffeNet* and *GoogLeNet* models fine-tuned according to the *conservative* and *adaptive* strategies (see Sec. 3.2.2). (Right) Accuracy of RLSC classifiers trained over features representations extracted from the 4 architectures considered in this work (see Sec. 3.2.1).

of these aspects in robot vision, taking iCubWorld as a testbed for our analysis. Note that in the following we use the term *instance* to refer to a specific object belonging to a given category, while *frame* denotes a single image depicting a scene or an object.

4.2.1 What do we gain by adding more frames?

We considered a 15-class categorization task on iCWT to compare the performance of learning models trained on an increasing number of examples. We created training sets of different size by sampling respectively $N = 10, 50, 150$ and 300 frames from each transformation sequence of an object. For each category (see the supplementary material for the list of categories) we used 7 objects for training, 2 for validation and 1 for test. Validation and test sets contained all images available for the corresponding instances. In order to account for statistical variability, we repeated these experiments for 10 trials, each time leaving out one different instance for testing. For this experiment we trained and tested on one of the two available days in iCWT (and one -the left- camera).

Fig. 6 reports the average classification accuracy of different learning models as more training examples are provided. Surprisingly, most architecture achieve remarkably high accuracy already when trained on the smallest training set and show little or no improvement when new data is available. This finding is in contrast with our expectations, since increasing the dataset size does not seem key to a significant improvement in performance.

Secondary observations:

- Fine-tuning and RLSC achieve comparable accuracy (both for *CaffeNet* and *GoogLeNet*).

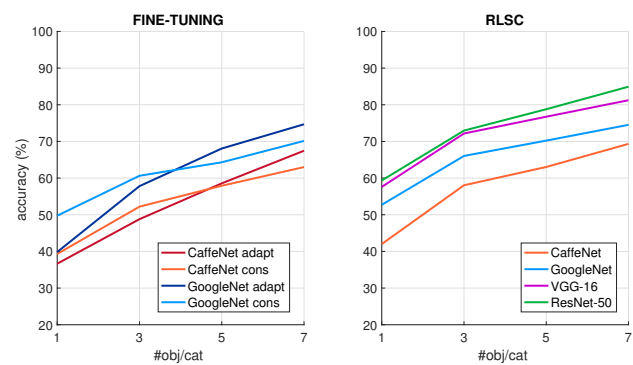


Fig. 7 Recognition accuracy vs # instances (number of object instances available during training). (Left) Accuracy of *CaffeNet* and *GoogLeNet* models fine-tuned according to the *conservative* and *adaptive* strategies (see Sec. 3.2.2). (Right) Accuracy of RLSC classifiers trained over features extracted from the 4 architectures considered in this work (see Sec. 3.2.1).

- We confirm the ILSVRC trends, with more recent networks outperforming older versions but with *VGG-16* features being better than those of *GoogLeNet* when using feature extraction with RLSC.
- Note that *CaffeNet* performs worse when training data is scarce because of the high number of parameters to be learned in the 3 FC layers (see Sec. 3 and the supplementary material).
- To further support these findings, in the supplementary material we report results for the same experiment performed using less example instances per category.

4.2.2 What do we gain by adding more instances?

We evaluated the impact of adding new object instances when training a recognition system. We consider this process as increasing the *semantic* variability of the training set, in contrast to increasing the *geometric* variability by showing more frames of a known object instance. We considered the same 15-class categorization task of Sec. 4.2.1 and created four training sets containing frames sampled from an increasing number of instances per category, namely 1, 3, 5 and 7. For all dataset, training data was randomly sub-sampled from all available transformation sequences to achieve identical total size of 900 images per category. Validation and test sets contained all frames for the remaining 2 and 1 instance (per category). We repeated the experiments for 10 trials.

Fig. 7 reports the accuracy of different models tested on this problem. Results show that increasing the semantic variability dramatically improves the accuracy of all models by a similar margin (around 15 – 20%).

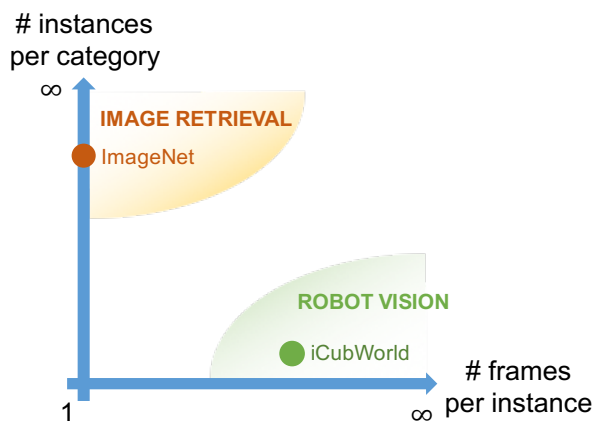


Fig. 8 Different training regimes from robot vision and image retrieval settings.

Moreover, from the observed trends we would expect these model to achieve even higher accuracy if more object instances were available.

Secondary observations:

- Fine-tuning the networks seems to lead to worse performance than RLSC on feature extraction both for *CaffeNet* and *GoogLeNet*.
- Also in this setting we confirm ILSVRC results, with more recent networks outperforming previous ones but with *VGG-16* outperforming *GoogLeNet* when using feature extraction with RLSC.
- To further support our findings, in the supplementary material we report results for a similar experiment but discriminating only between 10 or 5 categories.

4.2.3 Robot Vision and Image Retrieval

In this section we considered some of the main challenges associated to robot vision. While both robot vision and image retrieval address the same visual recognition problem, they are cast within two very different training regimes. We have identified here the two main causes of such difference (depicted in Fig. 8): 1) *semantic variability*, namely the amount of different object instances available for each category and 2) the amount of frames per instance.

Typically, in image retrieval settings a large number of images depicting different object instances for each category is available, but for each such instance very few images are provided. As an example, ILSVRC training set comprises ~ 1000 instances for each of the 1000 object categories, while only 1 image per instance is provided. On the opposite end of the spectrum, in robot vision settings it is easy to gather large amounts

of example images for a single instance (since the robot can move around and observe an object from multiple points of view). However there is a remarkable limitation in the total number of categories and instances that can be experienced.

Our analysis has shown that the limited availability of semantic variation that naturally occurs in robotics applications can dramatically affect the recognition accuracy of a learning system. Moreover, contrarily to our expectations, we observed that this limitation cannot be alleviated by simply feeding more training data (frames) to the network. Indeed, classifiers trained on datasets of different size (but same semantic variability) achieved identical performance. This can be extremely problematic since in robotics the overhead of collecting and acquiring examples of a novel instance is extremely expensive, while collecting more views of an object comes at a low cost. Unfortunately, we cannot adopt “data augmentation” strategies to artificially increase the semantic variability of a dataset as it is done for the case of view-point variability.

From our findings it appears clear that bridging the gap between robot vision and image retrieval needs a deeper analysis. To this end, in the following we deepen our analysis on the performance of CNNs on iCWT, with particular focus on the concept of invariance.

4.3 Invariance

In Sec. 4.2.1 we saw that models trained on few frames achieve comparable or even better accuracy to those trained larger datasets. These results suggest that the corresponding networks could leverage on a robust data representation and indeed in this section we investigate to what extent such models are invariant to the visual transformations in iCWT. Indeed, *invariance*, i.e. robustness to identity-preserving visual transformations of a scene, is a highly desirable behavior when designing and training a visual recognition system, since it can dramatically reduce the “complexity” of the learning problem (Anselmi et al 2016, 2015), increasing the capability of generalizing the visual appearance of an object category from a limited number of examples (ideally, just one). This is even more appealing in robotics applications where, usually, the robot is required to learn new objects on the fly, and recognize them reliably in unpredictable conditions.

To test the invariance of the CNNs, we considered again the 15-class categorization problem introduced in Sec. 4.2.2, where we used 7 object instances per category for training, 2 for validation and 1 for testing. However, we did not mix examples from all the five available sequences (*2D Rotation*, *3D Rotation*, *Scale*,



Fig. 9 Generalization performance across different visual transformations. Learning models were trained on one of the 5 transformations present in iCWT (specified in the horizontal axis), and then tested on all transformations. Accuracy is reported separately in each plot for each tested transformation. Shaded areas represent the improvement achieved by including all frames of a sequence instead of subsampling ~ 20 of them.

Background and *Mix*). Instead we performed training (and validation) using only an individual transformation, and then tested the learned model on the others. We repeated these experiments for 10 trials. We considered two “regimes”: one with including all images from a sequence, and another one subsampling images of a factor of 7 (as we did in Sec. 4.2.2, Fig. 7), since we previously observed that, while including more instances in the training set is important, including more frames is not.

As in Sec. 4.2.1 and 4.2.2, we limit our analysis to only one of the two available days in iCWT. Indeed, in this setting we aim to study the effect of isolated viewpoint transformations, without considering other nuisances due to, for example, the changes in the light and setting conditions that can appear from one day to another.

For this experiment we report only the accuracy of approaches that rely on the application of RLSC on top of feature representations extracted using off-the-shelf models (see Sec. 3.2.1). This is done to isolate the invariance properties of the networks trained on ImageNet. Note however that we performed these experiments also by fine-tuning the networks, as for previous tests, observing similar results.

Fig. 9 reports the generalization capabilities of models trained on a single transformation and tested on a different one. As a reference, we considered also a 6-th training set (*All*), obtained by randomly sampling points from all other 5 training sets, keeping similar size. This training set is analogous to those used in the experiments in Sec. 4.2.2 and 4.2.1 but with size reduced to be $\sim 150 * 7 = 1050$ images per category (and to only 150 images per category in the subsampled regime). We report the accuracy of the subsam-

pled training sets with a bold line, and the improvement achieved by considering all frames from the sequences with a shaded area of the same color.

We first confirm that adding example frames for a transformation does not significantly improve the networks’ invariance (even to the transformation itself). We then notice that overall the models exhibit invariance to transformations that have been included in the training set. It is worth noticing that in all cases the best performance are obtained when training and testing are performed on the same transformation and when all transformations are included in the training set (*All*). This demonstrates that enriching the dataset to include more transformations does not degrade performance.

Moreover, training on *Mix* achieves as good performance as *All* when tested on every specific transformation. This suggests that showing an object to the robot in a natural way, with all transformations appearing in random combinations, instead of systematically collecting sequences comprising individual transformations, is a feasible approach to obtain predictors invariant to these transformations.

It is interesting to note that rather different models trained on ImageNet exhibit the same invariance pattern. In particular, performance drops substantially when testing on a transformation that was not present on the training set. While this can be expected for transformations involving 3D rotations of the object, it is quite surprising for affine ones, namely *Scale*, *2D Rotation* and *Background* to which the convolutional structure of the CNN should be invariant “by design”, or learned during the training on ImageNet. We will further investigate this fact in Sec. 5.2, where we study the invariance of CNN models in the context of object *identification* rather than categorization.

5 Results (Object Identification)

So far in this work we focused on visual categorization problems, namely to assign a given object instance to the corresponding category. In this section we move instead to the task of object *identification* (or *instance recognition*), which consists in labeling a given image according to the object instance appearing in it. This problem is indeed very relevant to robotics settings, since reliable instance recognition skills would provide the system with finer control over tasks such as manipulation, grasping, etc. Also, considering a domestic scenario, the robot could be asked to use a *specific* object rather than *some* object in a category (e.g. “iCub, bring me *my* phone” instead of “a phone”).

Therefore, in parallel to the experiments on categorization, in this work we assessed the performance of Deep Learning methods on the task of object identification in robotics. Note that until recently, this problem has been approached with methods based on keypoints extraction and template matching (Lowe 2004; Philbin et al 2008; Collet et al 2011b; Crowley and Zisserman 2014; Collet et al 2011a, 2009; Muja et al 2011), however it has been recently observed that approaches relying on more holistic visual representations perform typically better in low/mid-resolution settings such as iCubWorld (Ciliberto et al 2013). Following this, in this section we will focus only on the CNN architectures considered in Sec. 3.

5.1 Knowledge Transfer: from Categorization to Identification

In Sec. 4.1 we have seen how knowledge acquired on ImageNet can be transferred to the iCubWorld domain to successfully tackle categorization tasks. A natural question is whether the same strategy would be similarly favorable for object identification. Indeed, in object identification settings there is no semantic variability (there is only one instance per class), but for categorization we have observed that semantic variability is extremely useful to the learning process (Sec. 4.2.2), while simply adding more images of a given instance is almost redundant (Sec. 4.2.1).

We addressed this question by considering an object identification task on iCWT, where we compared CNN models trained with an increasing number of examples. The setting is similar to the one used for categorization but for a 50-class object identification problem: we chose the 50 object instances from the *book*, *flower*, *glass*, *hairbrush* and *hairclip* categories, which do not appear in the ILSVRC dataset. We created four training sets containing respectively 10, 50, 150 and 300

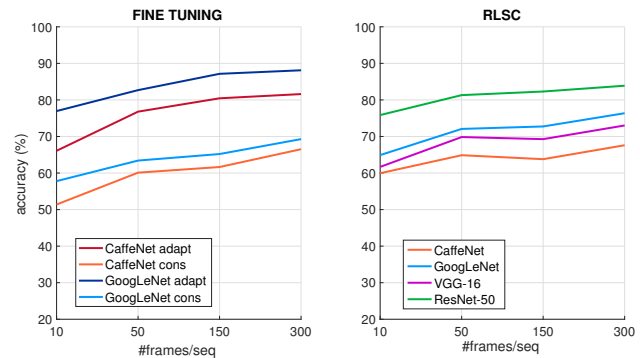


Fig. 10 Recognition accuracy vs # frames (Identification). (Left) Accuracy of *CaffeNet* and *GoogLeNet* models fine-tuned according to the *conservative* and *adaptive* strategies (see Sec. 3.2.2). (Right) Accuracy of RLSC classifiers trained over features representations extracted from the 4 architectures considered in this work (see Sec. 3.2.1).

images per object, sampled randomly from the 4 transformation sequences *2D Rot*, *3D Rot*, *Scale* and *Bkg* (see Sec. 2). From each dataset, 20% images were retained for model selection. The images from the *Mix* sequence were used to test the classification accuracy of the methods considered. As for the categorization experiment, only the images from a single day were used for these experiments.

Fig. 10 reports the average accuracy of CNN architectures trained on a growing number of examples. These results are in stark contrast with their counterpart on categorization (Sec. 4.2.1): we can clearly notice that adding more training data dramatically improves the recognition capabilities of all networks. This suggests that having access to more views of an instance allows the learning systems to create a more nuanced model of the object. Apparently, this richer model does not provide any advantage in categorization settings, but is extremely useful to recognize the same object in new images. In line with this observations, we notice also that in this setting the *adaptive* fine-tuning strategy significantly outperforms the competitors, suggesting that the representation learned for categorization on ImageNet, albeit already beneficial to the task, can be further improved to adapt to the object identification setting. These findings confirm and extend recent similar results from the instance retrieval literature (Babenko et al 2014; Gordo et al 2016).

5.2 Invariance

In Sec. 4.1, we have seen that the accuracy of an object identification system is greatly improved when it is provided with more examples of an instance. This observation seems to contradict the assumption that CNN are

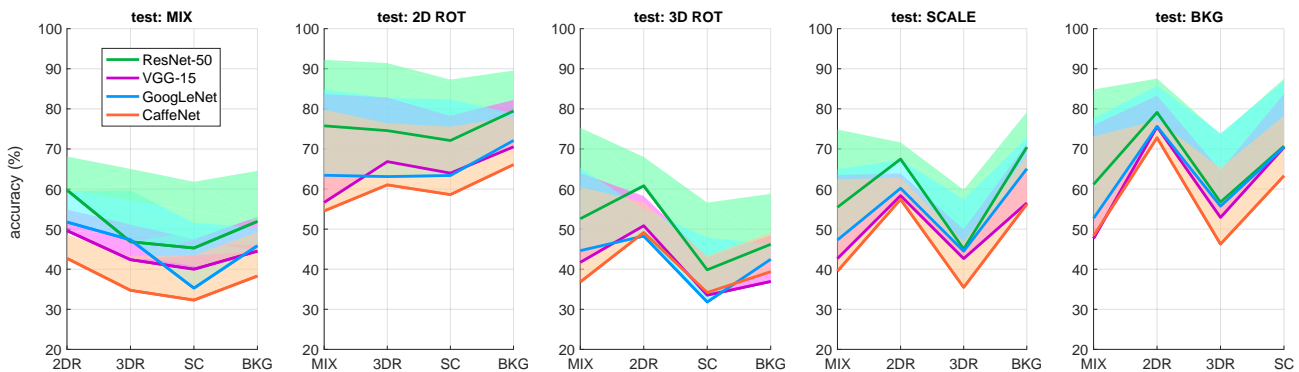


Fig. 11 Generalization performance across different visual transformations (Identification). RLSC are trained on one of the 5 transformations present in iCWT (specified in the horizontal axis), and then tested on the other transformations. Accuracy is reported separately in each plot for each tested transformation.

designed to be already invariant to view-point transformations. We addressed this question by considering a learning scenario similar to the one adopted in Sec. 4.3 to investigate invariance in categorization settings, but focused here on object identification. Specifically, we considered the same 50-class identification task, but restricted the training set to contain only images from a single transformation sequence of the 5 available in iCubWorld (Sec. 2). The resulting models were tested separately on the remaining transformations to assess the ability of the learning systems to generalize to new viewpoints. Similarly to Sec. 4.3 we considered only one day and evaluated only learning methods based on feature extraction (plus RLSC), in order to evaluate view-point invariance of off-the-shelf networks.

Fig. 11 reports the average accuracy of models trained a single transformation using respectively 10 or 150 frames per object and tested on another. We notice that the performance varies remarkably from one tested transformation to another, suggesting that the representations considered in these experiments are not invariant to transformations observed in iCWT. Interestingly, by comparing the two training regimes (i.e. large Vs small training set) we notice that the remarkable improvement observed in Sec. 5 when adding more frames is confirmed and extended also to the setting where the system is trained on a single transformation at the time. As expected, more recent networks significantly outperform previous models, with ResNet-50 achieving the highest accuracy by a large margin.

Similarly to what we observed in the categorization setting, Fig. 11 reports quite low performance when generalizing across transformations. In the following we discuss possible strategies to address this problem.

5.2.1 Improving the Invariance

In this section we consider different fine-tuning strategies to improve the invariance properties of off-the-shelf CNNs in identification settings. This analysis is motivated by the observation in Fig. 10 that *adaptive* fine-tuning performs significantly better than *conservative* and feature extraction based strategies. Indeed, this suggests that adapting the representation of the CNNs to the identification task is helpful to recognition, possibly because the network is actually learning the transformations to which it needs to be invariant. To this end, here we investigate whether fine-tuning a CNN on the iCubWorld domain can indeed improve/adapt the invariance properties of the network to the identification task. We have performed a preliminary set of experiments related to this question in (Pasquale et al 2016a), where we considered a smaller set of transformations and fine-tuning strategies, and focused only on the CaffeNet architecture.

We consider the same learning setting of the experiments reported in Fig. 11, but we evaluate learning models that are first “pre-fine-tuned” on one of the following datasets to improve their invariance:

- **iCubWorld identification (iCWT id).** This dataset contains images of all instances of the 5 object categories of iCWT that were not used in the previous experiments, namely *oven glove*, *squeezer*, *sprayer*, *body lotion* and *soda bottle*. Fine-tuning was performed with the *adaptive* strategy on the identification task. Training and validation sets were obtained following the same protocol of Sec. 5.1.
- **iCubWorld categorization (iCWT cat).** The same dataset as (iCW id) but fine-tuning was performed on the categorization task for the 5 objects

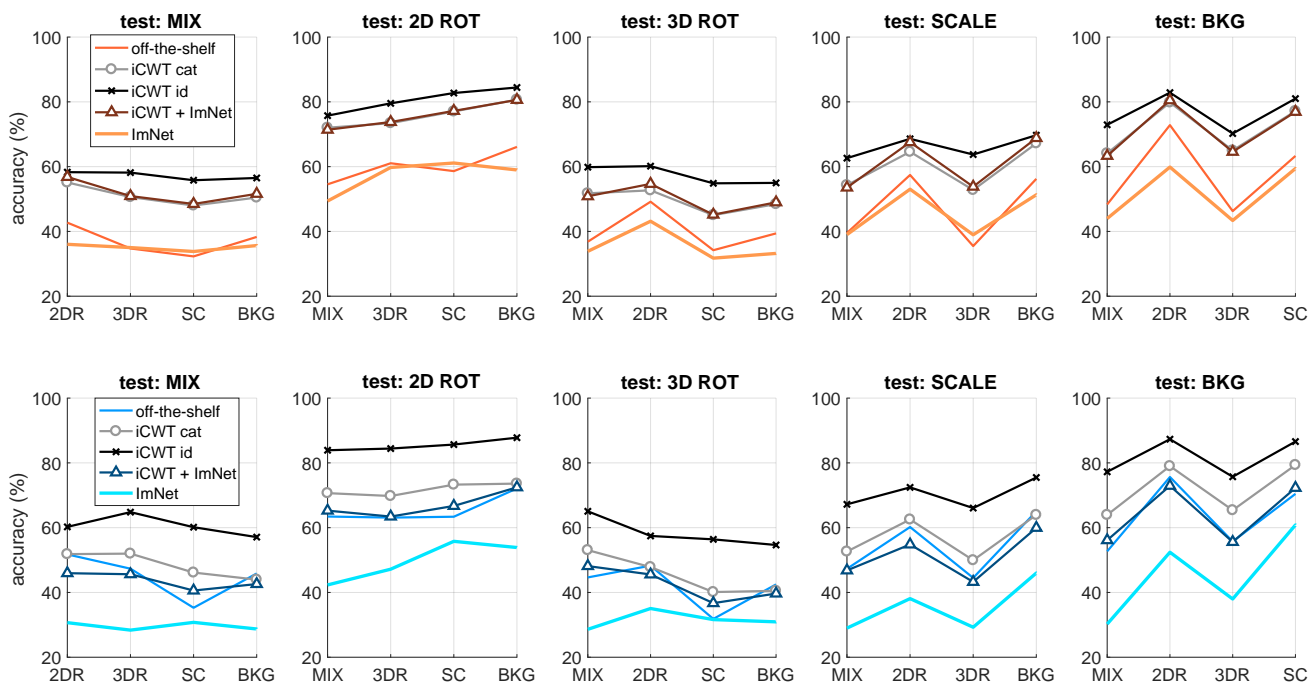


Fig. 12 Same experiment setting as in Fig. 11, but using different image representations, provided by *CaffeNet* (top, Orange) or *GoogLeNet* (bottom, Blue) network models fine-tuned according to different strategies (see Sec. 5.2.1).

considered. Again, the *adaptive* strategy was used. Train and validation sets were obtained following the same protocol as in Sec. 4.2.1.

- **iCubWorld + ImageNet (iCWT + ImNet).** This dataset contains images of the 5 categories above but sampled from both iCWT and ImageNet. Note that most iCWT categories do not appear in ILSVRC but are in synsets in the larger ImageNet dataset (see the supplementary material for a list of the corresponding synsets). All images in the synset were used. Fine-tuning was performed on the 5-class categorization task. This dataset is conceived to test the possibility to have the CNN directly learn the relation between ImageNet examples on which it has been originally trained and iCWT images.
- **ImageNet (ImNet).** This dataset contains the 5 ImageNet synsets corresponding to the 5 object categories on which the CNNs will be later trained and tested for invariance, namely *book*, *flower*, *glass*, *hairbrush* and *hairclip*. Fine-tuning was performed on the 5-class categorization task. This dataset allows the network to focus on data available on-line about the task at hand, but different from the images that the robot will observe.

Fig. 12 reports the accuracy of RLSC classifiers when trained on features extracted by the CNNs fine-tuned on the datasets described above. Training was performed separately for each transformation similarly to previ-

ous section, on the dataset containing only 10 example images per object instance. It can be noticed that pre-fine-tuning on the identification task is particularly advantageous, leading to a dramatic improvement over the model trained on off-the-shelf features. In particular, comparing these results with those in Fig. 11, we see that (iCWT id) trained on 10 examples per object performs on par with the off-the-shelf method trained on 150 images per object. Moreover, the performance of (iCWT id) are in general more stable across different viewpoint transformations, suggesting that the preliminary fine-tuning could have indeed allowed the CNNs to become partially invariant to transformations in iCubWorld. Interestingly the other CNNs do not provide similar improvements to identification and, in some cases, they even have worse performance than the off-the-shelf based classifier.

We conclude with a note related to categorization. Indeed, following these experiments we could wonder whether a similar pre-fine-tuning strategy could improve invariance also in the categorization setting of Sec. 4.3. However, empirical evidence showed that when performing fine-tuning on the datasets described above, the performance of the CNNs does not change significantly on the categorization task. We refer to the supplementary material for the analysis of this specific setting. We hypothesize this to be due to two possible reasons: 1) networks trained on the ILSVRC are already

highly optimized for categorization and there is no gain in adapting the visual representation or 2), the negative effect of the limited semantic variability in iCubWorld with respect to ImageNet may “overcome” the potential benefits of increasing the invariance to viewpoint transformations. This motivates some of the proposed directions of future investigation that we discuss in the following section.

6 Discussion and Future Work

In this work we studied the application of modern Deep Learning methods to visual recognition tasks in robotics. We challenged Deep Learning methods on an object recognition task that was specifically designed to represent a prototypical visual recognition problem in a real robotics application. Our experiments show that Deep Learning leads to remarkable performance for the visual tasks of object classification and instance recognition. Proper adoption of knowledge transfer strategies – in particular mixing Deep Learning with conventional “shallow” classifiers based on Kernel methods – plays a fundamental role, in that they leverage on the visual representation learned on large-scale datasets to achieve high performance in the robotic domain.

However, a substantial gap still exists between the performance that can be obtained on the two domains. Our analysis shows that this performance gap is due to scarce semantic variability, which characterizes the robotic domain and is due to the intrinsic cost of acquiring training samples. Yet, adoption of robotic systems in real applications requires to push further these requirements to achieve performance that approaches 100%. Indeed, in real-world robotics applications, failures due to object mis-detection or mis-classification can potentially lead to dramatically more critical and harmful consequences than in standard image retrieval scenarios. Therefore, the error rate of these systems will need to be as close as possible to zero to be considered for production and deployment in environments shared with humans.

In this section we consider possible directions for future research, aimed at mitigating the impact of such differences when performing visual recognition in robotics. The goal of our discussion is to consider them together in the same picture to present how, in our opinion, the robot vision problem could be addressed.

Improving invariance. The experiments in Sec. 4.3 show that models tested in this work are mostly *locally invariant*, namely their representation is robust to small view-point changes. While local invariance has been of main interest to computer vision in the past (Lowe

2004; Mikolajczyk and Schmid 2004), current research on invariance is instead focused on designing learning systems able to learn and encode representations that are robust to more dramatic (more “global”) transformations of an object (Anselmi et al 2016, 2015). Clearly, the more robust the visual representation is to viewpoint changes, small deformations, background variations etc., the less the corresponding model trained on an off-line large-scale dataset such as ImageNet will be biased to the specific training conditions. Research on invariant representations could therefore lead to both robust off-the-shelf robotics systems that do not need knowledge transfer and also allow to train on-the-fly classifier that can be trained from very few examples of a novel object and reliably recognize it from very different poses.

Multi-task learning. In this work we followed a typical approach to categorization, where no similarity or relation is assumed among different classes. However, in visual recognition settings object categories often have a number of visual features in common (e.g. wheels, windows, legs, handles and so on). Incorporating information about similarities across object classes within the learning model could significantly improve the overall accuracy of a recognition system, especially in presence of scarce training data. In particular, in the literature on multi-task learning there have been proposed several approaches to model relations across tasks (i.e. object categories) to directly enforce them on the learning problem when they are available a-priori (Crammer and Singer 2000; Micchelli and Pontil 2004; Evgeniou et al 2005; Joachims et al 2009; Fergus et al 2010; Lozano and Sindhvani 2011) or learn them when unknown (Argyriou et al 2008; Jacob et al 2008; Minh and Sindhvani 2011; Dinuzzo et al 2011; Sindhvani et al 2012; Ciliberto et al 2015a,b).

“Augmenting” the Semantic Variability. The simplest method for increasing semantic variability is to share data acquired in parallel from different robotic systems. Indeed, a similar strategy has been used to learn hand-eye coordination in a robotic setting, by training networks using data acquired in parallel by several robots (Levine et al 2016). Similarly, the Million Object Challenge (Oberlin et al 2015) aims to acquire a large dataset of object models by sharing data acquired from different laboratories owning a Baxter robot⁸. Along a similar direction we plan to extend iCubWorld with the help of the community of the iCub robot (at the time of writing more than 30 research groups in the world). Beyond expanding the dataset in

⁸ <http://www.rethinkrobotics.com/>

the direction of semantic variability, this would also allow to collect multiple acquisitions of the same object in different conditions, in order to extend the analysis presented in this work to nuisances like changes in the light and setting. Indeed, this is another critical aspect that we started to consider in the supplementary material of this work.

An alternative, or complementary approach is *data augmentation*. This method is often adopted in image retrieval settings to increase the viewpoint (and also illumination) variability during training by applying synthetic transformations to each image in the dataset (e.g. by rotating, flipping, cropping or changing the hue value). Visual augmentation to cope for semantic variability is a much more challenging problem, although recent work on *inverse graphics* (Mansinghka et al 2013; Kulkarni et al 2014, 2015) is a starting point in this direction.

Exploiting Contextual Information. Most work in visual recognition considers frames independently and rarely uses contextual information. A robot is typically exposed to a continuous stream of visual information, in which information is highly correlated. Exploiting these correlations can be done in many ways ranging from trivial solutions (like temporal averaging of the classification results) to more complex ones that rely on scene reconstruction and object tracking (Song et al 2015)).

Integrating 3D Information. In robotics, the problem of integrating 3D information with RGB has been recently investigated within a Deep Learning framework (Schwarz et al 2015; Redmon and Angelova 2015b). These results, although very promising, leverage only on off-the-shelf representations learned on large-scaled datasets of RGB-only images. In the future, the challenge will be to determine how to best encode and process 3D information within a CNN but also to acquire large-scale datasets for directly training such RGBD-based systems.

Self-supervised learning. One way to reduce the cost of supervision is to implement explorative strategies in which the robot autonomously interacts with the environment to collect training samples. Training instances in this scenario could be extracted autonomously by detecting invariances in the data which correspond to physical entities (e.g. coherent motion pattern (Wang and Gupta 2015) or bottom-up saliency cues). Strategies specific to the robotic domain could be devised by integrating multiple sensory modalities (Sinapov et al 2014b; Higy et al 2016) and a repertoire of explorative

actions designed specifically to extract these cues (like grasping or pushing objects (Montesano et al 2008; Fitzpatrick et al 2003; Hgman et al 2016; Pinto et al 2016)).

7 Conclusions

In this paper we have described a systematic study on the benefits of deep learning methods to robot vision. For our tests we have devised a prototypical vision task for a humanoid robot in which human-robot interaction is exploited to obtain realistic supervision and train an object recognition system. We presented the iCWT dataset and an in-depth investigation of the performance of state-of-the-art deep learning methods applied to our task. Our results confirm deep learning is a remarkable step forward. However, there is still a lot that needs to be done to reach the level of robustness and reliability required by real applications. We identified specific challenges and possible directions of research to bridge this gap. We are confident that the next few years will be rich of exciting progress in robotics.

Acknowledgements The work described in this paper is supported by the Center for Brains, Minds and Machines (CBMM), funded by NSF STC award CCF-1231216; and by FIRB project RBFR12M3AC, funded by the Italian Ministry of Education, University and Research. We gratefully acknowledge NVIDIA Corporation for the donation of the Tesla k40 GPU used for this research.

References

- Agrawal P, Girshick R, Malik J (2014) Analyzing the performance of multilayer neural networks for object recognition. In: Proceedings of the European Conference on Computer Vision (ECCV)
- Anselmi F, Leibo JZ, Rosasco L, Mutch J, Tacchetti A, Poggio T (2015) Unsupervised learning of invariant representations. Theoretical Computer Science DOI 10.1016/j.tcs.2015.06.048, URL <http://www.sciencedirect.com/science/article/pii/S0304397515005587>
- Anselmi F, Rosasco L, Poggio T (2016) On invariance and selectivity in representation learning. Information and Inference 5(2):134–158, URL <http://imaiai.oxfordjournals.org/content/5/2/134.full.pdf+html?sid=932cd117-4307-409b-9fc0-3acd9be20af0>
- Argyriou A, Evgeniou T, Pontil M (2008) Convex multi-task feature learning. Machine Learning 73
- Azizpour H, Razavian AS, Sullivan J, Maki A, Carlsson S (2015) From generic to specific deep representations for visual recognition. In: 2015 IEEE Conference on Computer Vision and Pattern Recognition Workshops (CVPRW), pp 36–45, DOI 10.1109/CVPRW.2015.7301270
- Babenko A, Slesarev A, Chigorin A, Lempitsky V (2014) Neural Codes for Image Retrieval, Springer International Publishing, Cham, pp 584–599. DOI 10.

- 1007/978-3-319-10590-1_38, URL http://dx.doi.org/10.1007/978-3-319-10590-1_38
- Baishya S, Bäumel B (2016) Robust material classification with a tactile skin using deep learning. In: IEEE International Conference on Intelligent Robots and Systems
- Bakry A, Elhoseiny M, El-Gaaly T, Elgammal A (2015) Digging Deep into the Layers of CNNs: In Search of How CNNs Achieve View Invariance. arXiv preprint pp 1–20, URL <http://arxiv.org/abs/1508.01983>, 1508.01983
- Bishop CM (2006) Pattern Recognition and Machine Learning (Information Science and Statistics). Springer-Verlag New York, Inc., Secaucus, NJ, USA
- Borji A, Izadi S, Itti L (2016) ilab-20m: A large-scale controlled object dataset to investigate deep learning. In: The IEEE Conference on Computer Vision and Pattern Recognition (CVPR)
- Bottou L (2012) Stochastic Gradient Tricks, vol 7700, Springer, p 430445. URL <https://www.microsoft.com/en-us/research/publication/stochastic-gradient-tricks/>
- Chatfield K, Simonyan K, Vedaldi A, Zisserman A (2014) Return of the devil in the details: Delving deep into convolutional nets. In: British Machine Vision Conference, 1405.3531
- Chitta S, Sturm J, Piccoli M, Burgard W (2011) Tactile Sensing for Mobile Manipulation. IEEE Transactions on Robotics 27(3):558–568, DOI 10.1109/TRO.2011.2134130
- Ciliberto C, Pattacini U, Natale L, Nori F, Metta G (2011) Reexamining lucas-kanade method for real-time independent motion detection: Application to the icub humanoid robot. In: 2011 IEEE/RSJ International Conference on Intelligent Robots and Systems, IEEE, pp 4154–4160
- Ciliberto C, Fanello SR, Natale L, Metta G (2012) A heteroscedastic approach to independent motion detection for actuated visual sensors. In: 2012 IEEE/RSJ International Conference on Intelligent Robots and Systems, IEEE, pp 3907–3913
- Ciliberto C, Fanello SR, Santoro M, Natale L, Metta G, Rosasco L (2013) On the impact of learning hierarchical representations for visual recognition in robotics. In: 2013 IEEE/RSJ International Conference on Intelligent Robots and Systems, pp 3759–3764, DOI 10.1109/IROS.2013.6696893
- Ciliberto C, Mroueh Y, Poggio T, Rosasco L (2015a) Convex learning of multiple tasks and their structure. In: International Conference on Machine Learning
- Ciliberto C, Rosasco L, Villa S (2015b) Learning multiple visual tasks while discovering their structure. In: Proceedings of the IEEE Conference on Computer Vision and Pattern Recognition, pp 131–139
- Collet A, Berenson D, Srinivasa SS, Ferguson D (2009) Object recognition and full pose registration from a single image for robotic manipulation. In: Robotics and Automation, 2009. ICRA'09. IEEE International Conference on, IEEE, pp 48–55
- Collet A, Martinez M, Srinivasa SS (2011a) The moped framework: Object recognition and pose estimation for manipulation. The International Journal of Robotics Research p 0278364911401765
- Collet A, Srinivasay SS, Hebert M (2011b) Structure discovery in multi-modal data: a region-based approach. In: Robotics and Automation (ICRA), 2011 IEEE International Conference on, IEEE, pp 5695–5702
- Crammer K, Singer Y (2000) On the learnability and design of output codes for multiclass problems. In: In Proceedings of the Thirteenth Annual Conference on Computational Learning Theory, pp 35–46
- Crowley E, Zisserman A (2014) The state of the art: Object retrieval in paintings using discriminative regions. In: BMVC
- Dahiya RS, Metta G, Valle M, Sandini G (2010) Tactile Sensing - From Humans to Humanoids. IEEE Transactions on Robotics 26(1):1–20, DOI 10.1109/TRO.2009.2033627
- Dansereau DG, Singh SP, Leitner J (2016) Interactive computational imaging for deformable object analysis. In: 2016 International Conference on Robotics and Automation (ICRA), IEEE
- Deng J, Dong W, Socher R, Li LJ, Li K, Fei-Fei L (2009) ImageNet: A Large-Scale Hierarchical Image Database. In: CVPR09
- Dinuzzo F, Ong CS, Gehler P, Pillonetto G (2011) Learning output kernels with block coordinate descent. International Conference on Machine Learning
- Donahue J, Jia Y, Vinyals O, Hoffman J, Zhang N, Tzeng E, Darrell T (2014) Decaf: A deep convolutional activation feature for generic visual recognition. In: Jebara T, Xing EP (eds) Proceedings of the 31st International Conference on Machine Learning (ICML-14), JMLR Workshop and Conference Proceedings, pp 647–655, URL <http://jmlr.org/proceedings/papers/v32/donahue14.pdf>
- Eitel A, Springenberg JT, Spinello L, Riedmiller M, Burgard W (2015) Multimodal deep learning for robust rgb-d object recognition. In: Intelligent Robots and Systems (IROS), 2015 IEEE/RSJ International Conference on, pp 681–687, DOI 10.1109/IROS.2015.7353446
- Everingham M, Van Gool L, Williams CKI, Winn J, Zisserman A (2010) The pascal visual object classes (voc) challenge. International Journal of Computer Vision 88(2):303–338, DOI 10.1007/s11263-009-0275-4, URL <http://dx.doi.org/10.1007/s11263-009-0275-4>
- Everingham M, Eslami SMA, Van Gool L, Williams CKI, Winn J, Zisserman A (2015) The pascal visual object classes challenge: A retrospective. International Journal of Computer Vision 111(1):98–136
- Evgeniou T, Micchelli CA, Pontil M (2005) Learning multiple tasks with kernel methods. In: Journal of Machine Learning Research, pp 615–637
- Fanello SR, Ciliberto C, Natale L, Metta G (2013a) Weakly supervised strategies for natural object recognition in robotics. IEEE International Conference on Robotics and Automation pp 4223–4229, DOI 10.1109/ICRA.2013.6631174
- Fanello SR, Ciliberto C, Santoro M, Natale L, Metta G, Rosasco L, Odone F (2013b) iCub World: Friendly Robots Help Building Good Vision Data-Sets. In: 2013 IEEE Conference on Computer Vision and Pattern Recognition Workshops, pp 700–705, DOI 10.1109/CVPRW.2013.106
- Fergus R, Bernal H, Weiss Y, Torralba A (2010) Semantic label sharing for learning with many categories. European Conference on Computer Vision
- Fitzpatrick P, Metta G, Natale L, Rao S, Sandini G (2003) Learning About Objects Through Action – Initial Steps Towards Artificial Cognition. vol 3, pp 3140–3145, DOI 10.1109/ROBOT.2003.1242036
- Fitzpatrick P, Needham A, Natale L, Metta G (2008) Shared challenges in object perception for robots and infants. Infant and Child Development 17(1):7–24
- Geusebroek JM, Burghouts GJ, Smeulders AW (2005) The amsterdam library of object images. International Journal of Computer Vision 61(1):103–112, DOI 10.1023/B:VISI.0000042993.50813.60, URL <http://dx.doi.org/10.1023/B:VISI.0000042993.50813.60>

- Goehring D, Hoffman J, Rodner E, Saenko K, Darrell T (2014) Interactive adaptation of real-time object detectors. In: Proceedings - IEEE International Conference on Robotics and Automation, IEEE, pp 1282–1289, DOI 10.1109/ICRA.2014.6907018
- Goodfellow I, Lee H, Le QV, Saxe A, Ng AY (2009) Measuring invariances in deep networks. In: Bengio Y, Schuurmans D, Lafferty JD, Williams CKI, Culotta A (eds) Advances in Neural Information Processing Systems 22, Curran Associates, Inc., pp 646–654, URL <http://papers.nips.cc/paper/3790-measuring-invariances-in-deep-networks.pdf>
- Goodfellow I, Bengio Y, Courville A (2016) Deep learning, URL <http://www.deeplearningbook.org>, book in preparation for MIT Press
- Gordo A, Almazán J, Revaud J, Larlus D (2016) Deep Image Retrieval: Learning Global Representations for Image Search, Springer International Publishing, Cham, pp 241–257. DOI 10.1007/978-3-319-46466-4_15, URL http://dx.doi.org/10.1007/978-3-319-46466-4_15
- Gorges N, Navarro SE, Gger D, Wrn H (2010) Haptic object recognition using passive joints and haptic key features. In: 2010 IEEE International Conference on Robotics and Automation, pp 2349–2355, DOI 10.1109/ROBOT.2010.5509553
- Griffin G, Holub A, Perona P (2007) Caltech-256 object category dataset. Tech. Rep. 7694, California Institute of Technology, URL <http://authors.library.caltech.edu/7694>
- He K, Zhang X, Ren S, Sun J (2015) Delving deep into rectifiers: Surpassing human-level performance on imagenet classification. In: The IEEE International Conference on Computer Vision (ICCV)
- He K, Zhang X, Ren S, Sun J (2016) Deep residual learning for image recognition. In: Computer Vision and Pattern Recognition (CVPR), 2016 IEEE Conference on
- Held D, Thrun S, Savarese S (2016) Robust single-view instance recognition. In: 2016 IEEE International Conference on Robotics and Automation (ICRA), pp 2152–2159, DOI 10.1109/ICRA.2016.7487365
- Herranz L, Jiang S, Li X (2016) Scene Recognition With CNNs: Objects, Scales and Dataset Bias. In: Conference on Computer Vision and Pattern Recognition, pp 571–579, DOI 10.1109/CVPR.2016.68
- Higy B, Ciliberto C, Rosasco L, Natale L (2016) Combining sensory modalities and exploratory procedures to improve haptic object recognition in robotics. In: IEEE-RAS International Conference on Humanoid Robots
- Hinton GE, Srivastava N, Krizhevsky A, Sutskever I, Salakhutdinov RR (2012) Improving neural networks by preventing co-adaptation of feature detectors. ArXiv e-prints [1207.0580](https://arxiv.org/abs/1207.0580)
- Hoffman J, Tzeng E, Donahue J, Jia Y, Saenko K, Darrell T (2013) One-Shot Adaptation of Supervised Deep Convolutional Models. ArXiv e-prints [1312.6204](https://arxiv.org/abs/1312.6204)
- Hosoda K, Iwase T (2010) Robust haptic recognition by anthropomorphic bionic hand through dynamic interaction. In: Intelligent Robots and Systems (IROS), 2010 IEEE/RSJ International Conference on, IEEE, pp 1236–1241
- Huh M, Agrawal P, Efros AA (2016) What makes ImageNet good for transfer learning? ArXiv e-prints [1608.08614](https://arxiv.org/abs/1608.08614)
- Hgman V, Bjrkmán M, Maki A, Kragic D (2016) A Sensorimotor Learning Framework for Object Categorization. IEEE Transactions on Cognitive and Developmental Systems 8(1):15–25, DOI 10.1109/TAMD.2015.2463728
- Ioffe S, Szegedy C (2015) Batch normalization: Accelerating deep network training by reducing internal covariate shift. vol 37, pp 448–456, URL <http://www.jmlr.org/proceedings/papers/v37/ioffe15>
- Jacob L, Bach F, Vert JP (2008) Clustered multi-task learning: a convex formulation. Advances in Neural Information Processing Systems
- Jia Y, Shelhamer E, Donahue J, Karayev S, Long J, Girshick R, Guadarrama S, Darrell T (2014) Caffe: Convolutional architecture for fast feature embedding. In: Proceedings of the ACM International Conference on Multimedia - MM '14, ACM Press, pp 675–678, DOI 10.1145/2647868.2654889
- Joachims T, Hofmann T, Yue Y, Yu CN (2009) Predicting structured objects with support vector machines. Commun ACM 52(11):97–104, DOI 10.1145/1592761.1592783, URL <http://doi.acm.org/10.1145/1592761.1592783>
- Kasper A, Xue Z, Dillmann R (2012) The kit object models database: An object model database for object recognition, localization and manipulation in service robotics. The International Journal of Robotics Research 31(8):927–934
- Kemp CC, Edsinger A, Torres-Jara E (2007) Challenges for robot manipulation in human environments [grand challenges of robotics]. IEEE Robotics Automation Magazine 14(1):20–29, DOI 10.1109/MRA.2007.339604
- Khosla A, Zhou T, Malisiewicz T, Efros AA, Torralba A (2012) Undoing the Damage of Dataset Bias, Springer Berlin Heidelberg, Berlin, Heidelberg, pp 158–171. DOI 10.1007/978-3-642-33718-5_12, URL http://dx.doi.org/10.1007/978-3-642-33718-5_12
- Kingma D, Ba J (2015) Adam: A Method for Stochastic Optimization. In: 3rd International Conference for Learning Representations (ICLR)
- Krizhevsky A, Sutskever I, Hinton G (2012a) Imagenet classification with deep convolutional neural networks. In: Advances in Neural Information Processing Systems, pp 1097–1105
- Krizhevsky A, Sutskever I, Hinton GE (2012b) Imagenet classification with deep convolutional neural networks. In: Pereira F, Burges CJC, Bottou L, Weinberger KQ (eds) Advances in Neural Information Processing Systems 25, Curran Associates, Inc., pp 1097–1105, URL <http://papers.nips.cc/paper/4824-imagenet-classification-with-deep-convolutional-neural-networks.pdf>
- Kulkarni TD, Mansinghka VK, Kohli P, Tenenbaum JB (2014) Inverse graphics with probabilistic cad models. arXiv preprint arXiv:14071339
- Kulkarni TD, Whitney WF, Kohli P, Tenenbaum J (2015) Deep convolutional inverse graphics network. In: Advances in Neural Information Processing Systems, pp 2539–2547
- Lai K, Bo L, Ren X, Fox D (2011) A large-scale hierarchical multi-view RGB-D object dataset. In: 2011 IEEE International Conference on Robotics and Automation, IEEE, pp 1817–1824, DOI 10.1109/ICRA.2011.5980382, URL <http://ieeexplore.ieee.org/articleDetails.jsp?arnumber=5980382>
- LeCun Y, Boser B, Denker JS, Henderson D, Howard RE, Hubbard W, Jackel LD (1989) Backpropagation applied to handwritten zip code recognition. Neural computation 1(4):541–551
- LeCun Y, Huang FJ, Bottou L (2004) Learning methods for generic object recognition with invariance to pose and lighting. In: Computer Vision and Pattern Recognition,

2004. CVPR 2004. Proceedings of the 2004 IEEE Computer Society Conference on, vol 2, pp II-97-104 Vol.2, DOI 10.1109/CVPR.2004.1315150
- Leitner J, Förster A, Schmidhuber J (2014) Improving robot vision models for object detection through interaction. In: 2014 International Joint Conference on Neural Networks (IJCNN), IEEE, pp 3355-3362
- Leitner J, Dansereau DG, Shirazi S, Corke P (2015) The need for more dynamic and active datasets. In: CVPR Workshop on The Future of Datasets in Computer Vision, IEEE
- Levine S, Pastor P, Krizhevsky A, Quillen D (2016) Learning Hand-Eye Coordination for Robotic Grasping with Deep Learning and Large-Scale Data Collection. arXiv:160302199 [cs] URL <http://arxiv.org/abs/1603.02199>, arXiv: 1603.02199
- Lowe DG (2004) Distinctive image features from scale-invariant keypoints. *International Journal of Computer Vision* 60(2):91-110, DOI 10.1023/B:VISI.0000029664.99615.94, URL <http://dx.doi.org/10.1023/B:VISI.0000029664.99615.94>
- Lozano A, Sindhvani V (2011) Block variable selection in multivariate regression and high-dimensional causal inference. *Advances in Neural Information Processing Systems*
- Mansinghka V, Kulkarni TD, Perov YN, Tenenbaum J (2013) Approximate bayesian image interpretation using generative probabilistic graphics programs. In: *Advances in Neural Information Processing Systems*, pp 1520-1528
- Meger D, Little JJ (2013) *The UBC Visual Robot Survey: A Benchmark for Robot Category Recognition*, Springer International Publishing, Heidelberg, pp 979-991. DOI 10.1007/978-3-319-00065-7_65, URL http://dx.doi.org/10.1007/978-3-319-00065-7_65
- Metta G, Sandini G, Natale L, Craighero L, Fadiga L (2006) Understanding mirror neurons: a bio-robotic approach. *Interaction studies* 7(2):197-232
- Metta G, Natale L, Nori F, Sandini G, Vernon D, Fadiga L, von Hofsten C, Rosander K, Lopes M, Santos-Victor J, Bernardino A, Montesano L (2010) The icub humanoid robot: an open-systems platform for research in cognitive development. *Neural networks : the official journal of the International Neural Network Society* 23(8-9):1125-34, DOI 10.1016/j.neunet.2010.08.010
- Micchelli CA, Pontil M (2004) Kernels for multi-task learning. *Advances in Neural Information Processing Systems*
- Mikolajczyk K, Schmid C (2004) Scale & affine invariant interest point detectors. *International journal of computer vision* 60(1):63-86, URL <http://link.springer.com/article/10.1023/B:VISI.0000027790.02288.f2>
- Minh HQ, Sindhvani V (2011) Vector-valued manifold regularization. *International Conference on Machine Learning*
- Model I, Shamir L (2015) Comparison of Data Set Bias in Object Recognition Benchmarks. *IEEE Access* 3:1953-1962, DOI 10.1109/ACCESS.2015.2491921, URL <http://ieeexplore.ieee.org/lpdocs/epic03/wrapper.htm?arnumber=7299607>
- Moldovan B, Moreno P, van Otterlo M, Santos-Victor J, De Raedt L (2012) Learning relational affordance models for robots in multi-object manipulation tasks. In: *Robotics and Automation (ICRA), 2012 IEEE International Conference on, IEEE*, pp 4373-4378
- Montesano L, Lopes M, Bernardino A, Santos-Victor J (2008) Learning object affordances: From sensory-motor coordination to imitation. *IEEE Transactions on Robotics* 24(1):15-26
- Muja M, Rusu RB, Bradski G, Lowe DG (2011) Rein-a fast, robust, scalable recognition infrastructure. In: *Robotics and Automation (ICRA), 2011 IEEE International Conference on, IEEE*, pp 2939-2946
- Natale L, Metta G, Sandini G (2004) Learning haptic representation of objects. URL <http://www.lira.dist.unige.it/projects/mirror/docs/thirdyear/papers/img04.pdf>
- Nene SA, Nayar SK, Murase H (1996) Columbia object image library (coil-100). Tech. rep.
- Nguyen A, Kanoulas D, Caldwell DG, Tsagarakis NG (2016) Detecting Object Affordances with Convolutional Neural Networks. In: *Intelligent Robots and Systems (IROS), 2016 IEEE/RJS International Conference on (to appear)*
- Oberlin J, Meier M, Kraska T, Tellex S (2015) Acquiring Object Experiences at Scale. In: *AAAI-RSS Special Workshop on the 50th Anniversary of Shakey: The Role of AI to Harmonize Robots and Humans*, blue Sky Award.
- Oquab M, Bottou L, Laptev I, Sivic J (2014) Learning and transferring mid-level image representations using convolutional neural networks. In: *The IEEE Conference on Computer Vision and Pattern Recognition (CVPR)*
- Pasquale G, Ciliberto C, Odone F, Rosasco L, Natale L (2015) Teaching iCub to recognize objects using deep Convolutional Neural Networks. vol 43, pp 21-25, URL <http://www.jmlr.org/proceedings/papers/v43/pasquale15>
- Pasquale G, Ciliberto C, Rosasco L, Natale L (2016a) Object Identification from Few Examples by Improving the Invariance of a Deep Convolutional Neural Network. In: *Intelligent Robots and Systems (IROS), 2016 IEEE/RJS International Conference on (to appear)*
- Pasquale G, Mar T, Ciliberto C, Rosasco LA, Natale L (2016b) Enabling depth-driven visual attention on the icub humanoid robot: Instructions for use and new perspectives. *Frontiers in Robotics and AI* 3(35), DOI 10.3389/frobt.2016.00035, URL http://www.frontiersin.org/humanoid_robotics/10.3389/frobt.2016.00035/abstract
- Philbin J, Chum O, Isard M, Sivic J, Zisserman A (2008) Lost in quantization: Improving particular object retrieval in large scale image databases. In: *Computer Vision and Pattern Recognition, 2008. CVPR 2008. IEEE Conference on, IEEE*, pp 1-8
- Pinto L, Gupta A (2015) Supersizing self-supervision: Learning to grasp from 50k tries and 700 robot hours. arXiv preprint arXiv:150906825 URL <http://arxiv.org/abs/1509.06825>
- Pinto L, Gupta A (2016) Supersizing self-supervision: Learning to grasp from 50k tries and 700 robot hours. In: *2016 IEEE International Conference on Robotics and Automation (ICRA)*, pp 3406-3413, DOI 10.1109/ICRA.2016.7487517
- Pinto L, Gandhi D, Han Y, Park YL, Gupta A (2016) The Curious Robot: Learning Visual Representations via Physical Interactions. arXiv:160401360 [cs] URL <http://arxiv.org/abs/1604.01360>, arXiv: 1604.01360
- Pinto N, Cox DD, DiCarlo JJ (2008) Why is real-world visual object recognition hard? *PLoS computational biology* 4(1):e27, DOI 10.1371/journal.pcbi.0040027, URL <http://journals.plos.org/ploscompbiol/article?id=10.1371/journal.pcbi.0040027>
- Ramisa A, Aldavert D, Vasudevan S, Toledo R, Lopez de Mantaras R (2011) The iiii30 mobile robot object recognition dataset. In: *Robotica* 2011
- Redmon J, Angelova A (2014) Real-Time Grasp Detection Using Convolutional Neural Networks. arXiv:14123128

- [cs] URL <http://arxiv.org/abs/1412.3128>, arXiv:1412.3128
- Redmon J, Angelova A (2015a) Real-time grasp detection using convolutional neural networks. In: 2015 IEEE International Conference on Robotics and Automation (ICRA), pp 1316–1322, DOI 10.1109/ICRA.2015.7139361
- Redmon J, Angelova A (2015b) Real-time grasp detection using convolutional neural networks. In: IEEE International Conference on Robotics and Automation, IEEE, pp 1316–1322, URL http://ieeexplore.ieee.org/xpls/abs_all.jsp?arnumber=7139361
- Rennie C, Shome R, Bekris KE, Ferreira De Souza A (2016) A dataset for improved rgb-d based object detection and pose estimation for warehouse pick-and-place. IEEE Robotics and Automation Letters (RA-L) [Also accepted to appear at the 2016 IEEE International Conference on Robotics and Automation (ICRA)] 1:1179–1185, URL http://www.cs.rutgers.edu/~kb572/pubs/icra16_pose_estimation.pdf
- Rivera-Rubio J, Idrees S, Alexiou I, Hadjilucas L, Bharath AA (2014) Small hand-held object recognition test (SHORT). In: 2014 IEEE Winter Conference on Applications of Computer Vision (WACV), pp 524–531, DOI 10.1109/WACV.2014.6836057
- Rodner E, Hoffman J, Donahue J, Darrell T, Saenko K (2013) Towards Adapting ImageNet to Reality: Scalable Domain Adaptation with Implicit Low-rank Transformations. ArXiv e-prints 1308.4200
- Rudi A, Camoriano R, Rosasco L (2015) Less is more: Nystrom computational regularization. In: Advances in Neural Information Processing Systems, pp 1648–1656
- Rudi A, Camoriano R, Rosasco L (2016) Generalization properties of learning with random features. arXiv preprint arXiv:160204474
- Russakovsky O, Deng J, Su H, Krause J, Satheesh S, Ma S, Huang Z, Karpathy A, Khosla A, Bernstein M, Berg AC, Fei-Fei L (2015) Imagenet large scale visual recognition challenge. International Journal of Computer Vision 115(3):211–252, DOI 10.1007/s11263-015-0816-y, URL <http://dx.doi.org/10.1007/s11263-015-0816-y>
- Schwarz M, Schulz H, Behnke S (2015) Rgb-d object recognition and pose estimation based on pre-trained convolutional neural network features. In: 2015 IEEE International Conference on Robotics and Automation (ICRA), pp 1329–1335, DOI 10.1109/ICRA.2015.7139363
- Simonyan K, Zisserman A (2015) Very deep convolutional networks for large-scale image recognition. In: International Conference on Learning Representations
- Sinapov J, Schenck C, Staley K, Sukhoy V, Stoytchev A (2014a) Grounding semantic categories in behavioral interactions: Experiments with 100 objects. Robotics and Autonomous Systems 62(5):632–645, DOI 10.1016/j.robot.2012.10.007, URL <http://linkinghub.elsevier.com/retrieve/pii/S092188901200190X>
- Sinapov J, Schenck C, Stoytchev A (2014b) Learning relational object categories using behavioral exploration and multimodal perception. In: IEEE International Conference on Robotics and Automation, IEEE, pp 5691–5698, URL http://ieeexplore.ieee.org/xpls/abs_all.jsp?arnumber=6907696
- Sindhvani V, Lozano AC, Minh HQ (2012) Scalable matrix-valued kernel learning and high-dimensional nonlinear causal inference. CoRR abs/1210.4792
- Singh A, Sha J, Narayan KS, Achim T, Abbeel P (2014) Big-bird: A large-scale 3d database of object instances. In: 2014 IEEE International Conference on Robotics and Automation (ICRA), pp 509–516, DOI 10.1109/ICRA.2014.6906903
- Song S, Zhang L, Xiao J (2015) Robot In a Room: Toward Perfect Object Recognition in Closed Environments. arXiv:150702703 [cs] URL <http://arxiv.org/abs/1507.02703>, arXiv: 1507.02703
- Srivastava N, Hinton G, Krizhevsky A, Sutskever I, Salakhutdinov R (2014) Dropout: A simple way to prevent neural networks from overfitting. Journal of Machine Learning Research 15:1929–1958, URL <http://jmlr.org/papers/v15/srivastava14a.html>
- Stamos D, Martelli S, Nabi M, McDonald A, Murino V, Pontil M (2015) Learning with dataset bias in latent subcategory models. In: Proceedings of the IEEE Computer Society Conference on Computer Vision and Pattern Recognition, IEEE, vol 07-12-June, pp 3650–3658, DOI 10.1109/CVPR.2015.7298988, URL <http://ieeexplore.ieee.org/lpdocs/epic03/wrapper.htm?arnumber=7298988>
- Sünderhauf N, Shirazi S, Dayoub F, Upcroft B, Milford M (2015) On the performance of convnet features for place recognition. In: Intelligent Robots and Systems (IROS), 2015 IEEE/RSJ International Conference on, pp 4297–4304, DOI 10.1109/IROS.2015.7353986
- Sünderhauf N, Dayoub F, McMahon S, Talbot B, Schulz R, Corke P, Wyeth G, Upcroft B, Milford M (2016) Place categorization and semantic mapping on a mobile robot. In: 2016 IEEE International Conference on Robotics and Automation (ICRA), pp 5729–5736, DOI 10.1109/ICRA.2016.7487796
- Szegedy C, Liu W, Jia Y, Sermanet P, Reed S, Anguelov D, Erhan D, Vanhoucke V, Rabinovich A (2015) Going deeper with convolutions. In: The IEEE Conference on Computer Vision and Pattern Recognition (CVPR)
- Tommasi T, Patricia N, Caputo B, Tuytelaars T (2015) A deeper look at dataset bias. In: Lecture Notes in Computer Science (including subseries Lecture Notes in Artificial Intelligence and Lecture Notes in Bioinformatics), Springer International Publishing, vol 9358, pp 504–516, DOI 10.1007/978-3-319-24947-6_42
- Torralba A, Efros AA (2011) Unbiased look at dataset bias. In: Proceedings of the IEEE Computer Society Conference on Computer Vision and Pattern Recognition, pp 1521–1528, DOI 10.1109/CVPR.2011.5995347
- Wang X, Gupta A (2015) Unsupervised Learning of Visual Representations using Videos. arXiv:150500687 [cs] URL <http://arxiv.org/abs/1505.00687>, arXiv: 1505.00687
- Xiang Y, Mottaghi R, Savarese S (2014) Beyond pascal: A benchmark for 3d object detection in the wild. In: IEEE Winter Conference on Applications of Computer Vision, pp 75–82, DOI 10.1109/WACV.2014.6836101
- Yosinski J, Clune J, Bengio Y, Lipson H (2014) How transferable are features in deep neural networks? In: Advances in Neural Information Processing Systems, pp 3320–3328
- Zeiler MD, Fergus R (2014) Visualizing and Understanding Convolutional Networks, Springer International Publishing, Cham, pp 818–833. DOI 10.1007/978-3-319-10590-1_53, URL http://dx.doi.org/10.1007/978-3-319-10590-1_53

Are we Done with Object Recognition? The iCub robot’s Perspective. Supplementary Material

Giulia Pasquale, Carlo Ciliberto, Francesca Odone, Lorenzo Rosasco and Lorenzo Natale

A iCubWorld Transformations

Fig. 13 reports one image for each object *instance* in the iCWT dataset. We report also the reference number of the associated synset in ImageNet (Russakovsky et al 2015). Note that not all categories in iCWT are part of the ILSVRC, but they belong (or at least are similar) to synsets in the larger ImageNet dataset (Deng et al 2009).

B Off-the-shelf CNNs

In Sec. 4.1 we observed that direct application of off-the-shelf CNNs to iCubWorld leads to poor performance. In this section we provide some additional details on the experiment that we reported in Fig. 5.

B.1 Image Preprocessing

When applying deep CNNs to our setting, we first evaluated the impact of considering coarser or finer regions around the object in the images. Indeed, each image in iCWT is annotated with the coordinates of the object’s centroid and with a bounding box provided by segmentation of the depth map (see Sec. 2.1). We took advantage of this rough localization in order to avoid considering full images for classification and we compared different strategies to extract a crop from the images. Specifically, we tried either to extract a square crop of fixed radius, just by using the information on the centroid, or to use the bounding box provided by the routine segmenting the depth map (i.e., the smallest rectangle enclosing the object’s blob). In both cases we tried two sizes: using a radius of 256 or 384 for the square crop, and leaving a margin of 30 or 60 pixels around the depth’s bounding box.

Then, since deep CNNs require a fixed sized input (227×227 for *CaffeNet* and 224×224 for the other considered models), different preprocessing strategies can be applied in order to feed an image to a network. We reproduced the operations that are specified at the reference page of each particular CAFFE model. For convenience we report them in Tab. 4. These, in general, consist in the subtraction of the mean image (or the mean pixel value) of the dataset on which the model has been trained and in the extraction of a grid of crops (eventually at multiple scales as for *VGG-16*) of the required size. Usually, the final prediction is computed by aggregating the predictions of more crops to gain robustness. However, since in our case the image is in fact already a crop around the object, we compared the advantage of this grid approach against just considering the central crop (and a single scale in the case of *VGG-16*).

Fig. 14 reports the results of Sec. 4.1, Fig. 5, but obtained by testing off-the-shelf CNNs on iCWT with the different described strategies. It can be noticed that performing a finer

Table 4 Preprocessing operations executed on images before feeding the networks.

Model	Mean Subtraction	Scaling	Crop Extraction
CaffeNet ResNet-50	image	mean image size (256×256)	2×2 grid + center mirrored
GoogLeNet	pixel	256×256	2×2 grid + center mirrored
VGG-16	pixel	shorter side to 256, 384, 512	5×5 grid at each scale mirrored

localization of the object in the image (Blue and Green) provides better performance for all architectures. Also, considering more than the central crop provides a little advantage (for *VGG-16* this is even detrimental). This is reasonable because we already localized the object and we are in fact considering a portion of the image.

We finally chose to apply CNNs by extracting a square region of 256×256 from iCWT images, and then considering only the central crop (Light Green in Fig. 14). Hence, we did not need to scale the image (for *VGG-16* we considered a single scale). This is the same performance reported, for instance, in Fig. 5 (Dark Blue) and the strategy used in all experiments. We chose to extract fixed-size regions, instead of relying on the bounding box of the depth map, since we aimed at evaluating, in the following of our analysis, also invariance properties to geometric transformations (as, e.g, scaling). We precise that when applying the networks to ImageNet instead, we used the multi-crop strategy suggested for each of the architectures (see Tab. 4).

B.2 1000-class Categorization Results

In Fig. 5 we reported the accuracy of the off-the-shelf CNNs applied on iCWT and ImageNet. However, since the task was reduced to a 11-class categorization setting, we considered the prediction of the networks limited to the 11 corresponding labels rather than the full vector of 1000 scores normally produced by a CNN trained on the ILSVRC. For completeness, in Fig. 15 we report the resulting accuracy of the same CNNs but taking as prediction the class achieving maximum score over all available 1000, even if not present in the considered test sets (the one of iCWT and the reduced ImageNet). As can be noticed, performance drops even below chance on iCWT (since now the “real” chance is $1/1000$ rather $1/11$).

B.3 Viewpoint Biases

In this section we follow-up the preliminary analysis reported in Sec. 4.1 discussing the potential biases in ImageNet, pre-



Fig. 13 Example images for the 200 objects in iCubWorld Transformations.

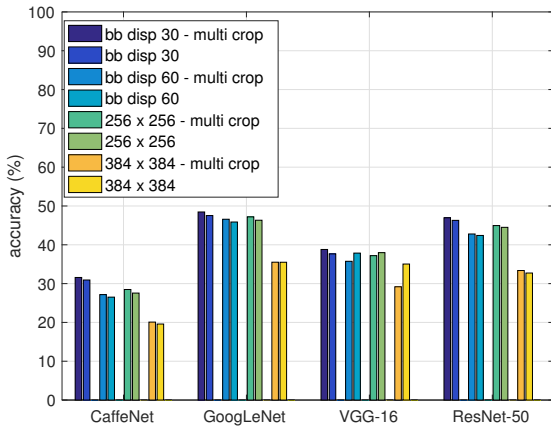


Fig. 14 Average classification accuracy of off-the-shelf networks tested on iCWT segmenting the object according to different strategies.

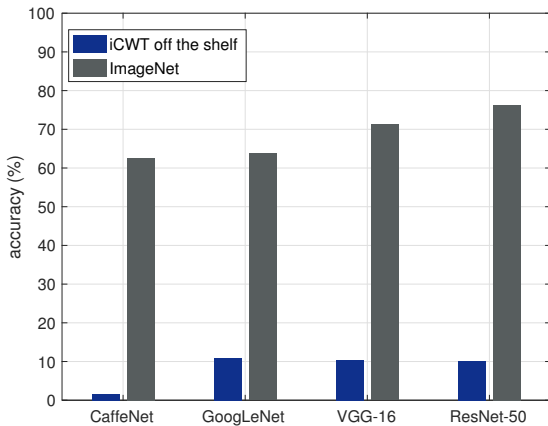


Fig. 15 Average classification accuracy of off-the-shelf networks (trained on ILSVRC) tested on iCWT (Dark Blue) or on ImageNet itself (Gray). The test sets for the two datasets are restricted to the 11 shared categories (see Sec. 2).

venting off-the-shelf models to generalize well when tested on iCubWorld without applying knowledge transfer techniques. To this end, we report a series of excerpts showing the frame-by-frame predictions of some of the CNNs considered when tested on iCWT sequences. This qualitative analysis allows to better understand what frames of iCubWorld are actually “harder” to recognize for the CNNs and compare them with prototypical examples in ImageNet.

We report here the predictions obtained by using *GoogLeNet*, but we made similar observations for the other architectures. As in Fig. 5, the prediction was computed as the maximum score among those of 11 the classes present in test set, rather than the full vector of 1000. We restricted the analysis to a subset of the test set considered in Fig. 5: specifically, to the 5 best recognized categories and two specific visual transformations: *Scale* and *2D Rotation*.

In Fig. 16 we report frame-by-frame predictions on sequences containing the *Scale* transformation separately for each category. In each plot, we represent the sequences of

the 10 object instances of that category as rows of a matrix (the temporal dimension, or frame index, is reported in the horizontal axis). In each row, the frame-by-frame predictions over the sequence are represented as vertical bars: *White* if the prediction is correct, *Red* if it is wrong (and *Black* if the sequence is terminated). It can be noted that, since during the acquisition the operator was moving the object back and forth in front of the robot, starting close and slowly moving backward (eventually re-approaching the robot in some sequences), the CNN manages to recognize the object only when this appears at a relatively large scale (white bars mostly concentrated in the first half of rows). This qualitative observation confirms recent studies (Herranz et al 2016) that specifically highlight the problem of the scale bias in CNNs, preventing models trained on object-centric datasets as ImageNet to generalize to scene-centric settings, where objects mostly appear in a small part of the image (like in the second part of our sequences).

In Fig. 17 we report the same for sequences containing *2D Rotation*. In this case, the operator was rotating the object (always maintaining the same face visible to the robot) at a constant speed. Indeed, it can be noticed that on many sequences there are periodic time intervals when the CNN does (or does not) recognize the object, corresponding to configurations in which that category appears more or less frequently in the ImageNet dataset. For example, we observed that soap dispensers and mugs in ImageNet are mostly placed on tables, and consequently are never recognized when they are, e.g. upside-down.

C Model (Pre) Selection

In this section we provide details regarding the parameter selection of the learning methods adopted in this work and described in Sec. 3.2.

C.1 Feature Extraction and RLSC

Here we specify the design choices that we made to implement each of the steps described in Sec. 3.2.1.

When feeding images to the networks in order to extract their representation, we applied the preprocessing pipeline that was explained and motivated in Sec. B.1. For each architecture, the layers considered as output to extract such representations, were specified in Tab. 2. For *CaffeNet* and *VGG-16* we indicated either *fc6* or *fc7* layers, since these networks have more than one FC layer that can provide 1-dimensional output representations of the full image, the best choice depending on the application. We then resorted to (Rudi et al 2015) for the Nystrom subsampling approach that we used to implement the Gaussian RLSC. This algorithm in fact involves determining some hyperparameters, the most critical being the number m of training examples to subsample to approximate the kernel matrix.

In order to evaluate the best output layer for *CaffeNet* and *VGG-16*, and also to assign a reasonable value to m , we considered one small and one large categorization tasks on iCWT, representative of the smallest and larger task that we expected to run in our analysis, and compared the RLSC accuracy on them when varying these factors.

We fixed a 15-class categorization problem, training on 7 object instances per category and validating on 2. For each

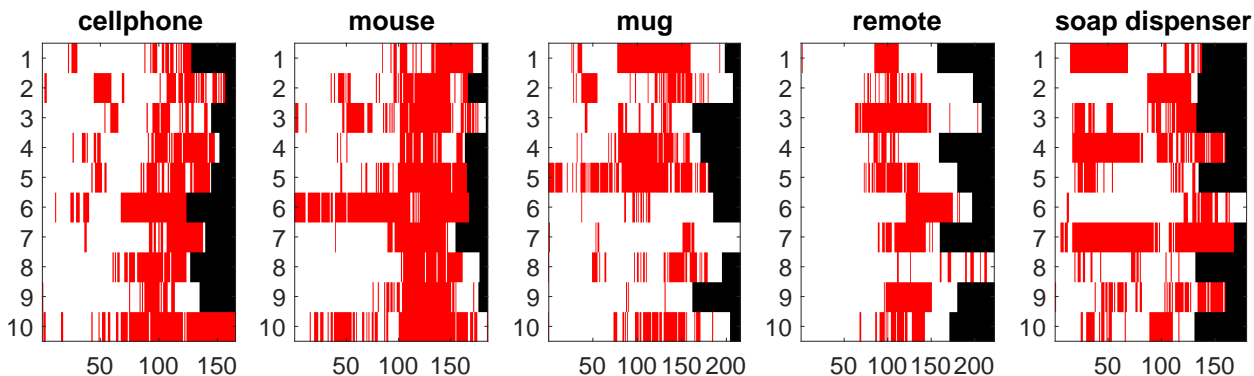


Fig. 16 Frame-by-frame predictions of *GoogLeNet* on image sequences containing the *Scale* transformation, reported for 5 categories in different plots. The sequences of the 10 object instances belonging to each category are represented as matrix rows (the temporal dimension, or frame index, is reported in the horizontal axis). In each row, the frame-by-frame predictions over the sequence are represented as vertical bars: *White* if the prediction is correct, *Red* if it is wrong (and *Black* if the sequence is terminated).

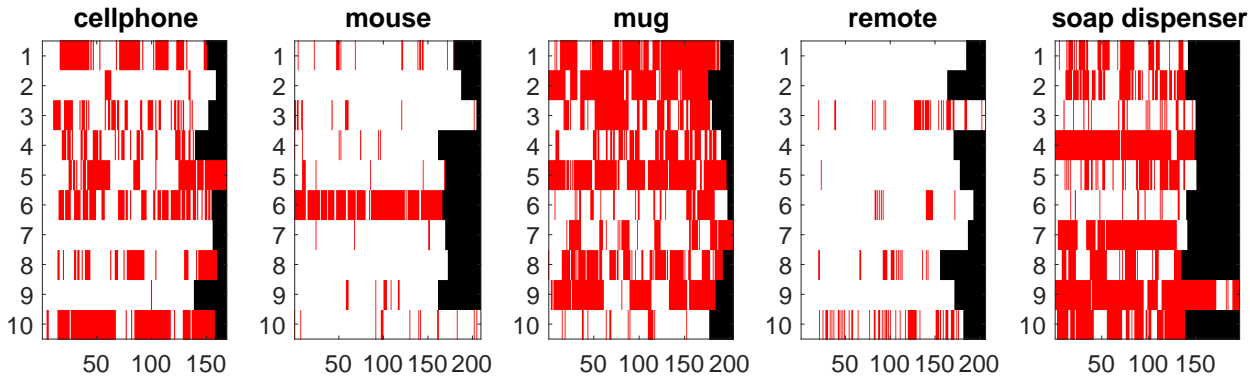


Fig. 17 Same as Fig. 16, but on image sequences containing *2D Rotation*.

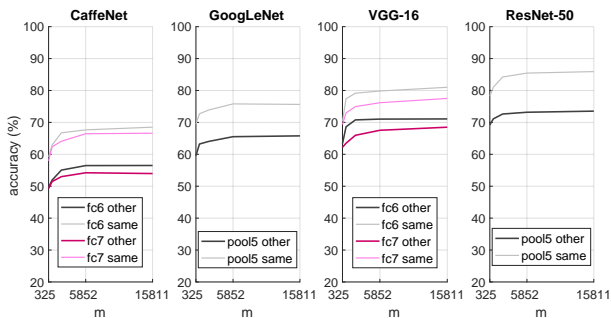


Fig. 18 Classification accuracy reported by training RLSC over image representations extracted by the four considered architectures. A “large” categorization experiment is performed (with $\sim N = 95000$ training examples) and m is varied between \sqrt{N} and 15000 (horizontal axis). Performance on the same training day (Light colors) and on another one (Dark colors) is reported.

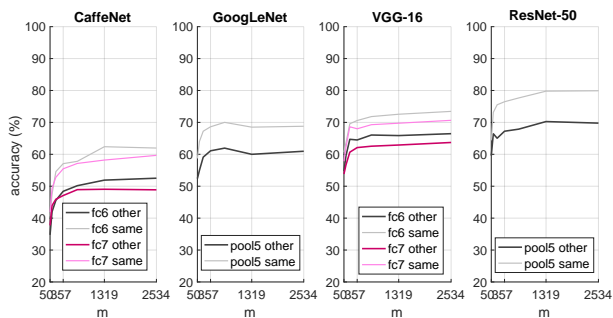


Fig. 19 Similar to Fig. 18 but on a “small” categorization experiment ($\sim N = 2500$ training examples), varying m between \sqrt{N} and N .

instance, we considered the sequences of all 5 visual transformations and one camera. We considered only one day, among

the two available in iCWT, for training, and tested on the instance left out from the training set, in both days. For the large task, we considered all frames per sequence, leading to ~ 6300 training examples per class, whereas for the small task we subsampled ~ 4 frames per sequence, leading to ~ 170 examples per class (similarly to what we did in Sec. 4.2.1).

Fig. 19 and 18 reports the average accuracy respectively for the small and large experiment. We performed the two experiments using the representations from the four considered architectures (reported separately), using either *fc6* layer (Gray) or *fc7* (Pink) for *CaffeNet* and *VGG-16*. In each case, we increased logarithmically the value of m (horizontal axis) starting from \sqrt{N} , N being the size of the training set. For the small experiment we stopped at N , whereas for the large experiment we stopped at values where we observed very little performance improvements with respect to much longer training times. The performance on the same day on which we trained is reported in Light (Gray/Pink), whereas the performance on the other day is reported in Dark colors.

We first observed that *fc6* features consistently performed better than *fc7*, hence we decided to use this layer when extracting representations from off-the-shelf *CaffeNet* or *VGG-16* on images of iCWT. Then, we also observed that relatively small values of m could provide good accuracies and therefore we chose to fix $m = \min(15000, N)$ in all experiments.

It is worth noting that we performed a similar empirical analysis to the one reported here in order to assess the best output layer to use to extract visual representations from the models of Sec. 5.2.1 and D.3 that were previously fine-tuned on subsets of iCWT. In that case, we observed that *fc7* features were providing the best performance and therefore we used this layer in our experiments in those sections. This can be explained considering that “more specialized” features can be extracted from models that have been adapted to our setting, while “more general” features of off-the-shelf models provide better generalization performance on iCWT.

C.2 Fine-tuning

In this section we provide details on how we performed the fine-tuning procedure and on the choice of the two strategies, *adaptive* and *conservative*, reported in Tab. 3.

C.2.1 General Protocol

The image preprocessing pipeline was similar to the one reported in Sec. B.1: once a square 256×256 region around the object’s centroid was extracted, we either subtracted the mean image (*CaffeNet*) or pixel (*GoogLeNet*) of the training set.

When training, the rest of processing was performed within CAFFE, specifically extracting a random 227×227 crop (randomly mirrored horizontally) before passing it to the network. At test phase, the prediction over one image was taken by extracting the central crop instead of a random one (see Sec. B.1).

The training set was shuffled before starting the fine-tuning process since we observed that similarity of images within a batch negatively affected convergence of the back-propagation algorithm. When fine-tuning a network, we evaluated the model’s performance on a validation set every epoch and we finally chose the epoch achieving highest validation accuracy.

We left the batch size to the values specified in CAFFE (and reported in Tab. 3). The number of iterations – or, equivalently, of epochs – was fixed empirically, observing that in general the performance was saturating after 6 epochs for all models but for *conservative* fine-tuning of *CaffeNet*, that involves the learning of all parameters of the 3 FC layers and

therefore takes more time to converge. In this case, we fixed the number of epochs to ~ 36 .

C.2.2 Hyperparameters Choice

In this section we report on the empirical analysis that we performed in order to understand the effect and the relative importance of the hyperparameters involved in fine-tuning deep architectures as *CaffeNet* or *GoogLeNet* in our scenario.

While model selection is per se an open problem when dealing with deep networks, in our setting this issue is even more complicated by the fact that we do not have a fixed reference task on which to optimize the training (as e.g., can be the ILSVRC), but we instead plan to span over wide range of tasks, comprising small or large training sets. Indeed, the study presented in this work aims at comparing models trained on different categories, objects, transformations, and so forth.

We considered therefore the same two experiments that we used to perform parameter selection for the RLSC approach (the “small” and “large” categorization tasks described in Sec. C.1) and we fine-tuned *CaffeNet* and *GoogLeNet* on them by varying the values of multiple hyperparameters. In the following, we report this analysis separately for the two architectures.

CaffeNet. We considered the parameters appearing in Tab. 3 and varied the value of each of them in the following way:

Base LR: the starting learning rate of the layers that are initialized with the parameters of the off-the-shelf model.

We tried $10^{-3}, 5 * 10^{-4}, 10^{-4}, 5 * 10^{-5}, 10^{-5}, 10^{-6}, 0$.

Learned FC Layers: which fully-connected (FC) layers are from

scratch and their specific starting LR. We tried to learn (i) only *fc8* with starting LR set to 10^{-2} , or (ii) including also *fc7* and (iii) finally also *fc6*. As an empirical rule, every time we included one more layer to learn from scratch, we decreased the starting LR of these layers of a factor of 10 (hence 10^{-3} in (ii) and 10^{-4} in (iii)).

Dropout %: percentage of dropout in FC layers. We tried 50% (default CAFFE value) or 65%.

Solver: the algorithm used for the stochastic gradient descent. We used the *SGD* solver (Bottou 2012) in CAFFE.

LR Decay Policy: the decay rate of the learning rates. We tried either polynomial decay with exponent 0.5 or -3 , or step decay decreasing the LR of a factor of 10 every 2 epochs.

We tried all possible combinations of values. For the parameters that are missing here, we kept their value as specified in *Caffe* reference models (see also the previous section).

We observed that the dropout percentage had a small influence and left it to the default value. We also observed that the polynomial decay with smaller slope was consistently better (of $\sim 5 - 10\%$ accuracy). The most critical parameters were instead the base LR and the numbers of FC layers learned from scratch. In Fig. 20 we report as an example the accuracy obtained respectively when learning only *fc8* (Left) or *fc6, fc7* and *fc8* (Right). In each case, we decreased the base LR of all other layers from 10^{-3} to 0 (horizontal axis). Performance is reported, as in Fig. 19 and 18, for both the same day of training (Light Gray) and a different one (Dark Gray). While we tried all values of base learning rate on the “small” experiment (Continuous Line), for the “large” experiment we chose one small, medium and large value (Dots).

For interpreting the results, it can be useful to recall that the strategy that learns from scratch the three FC layers

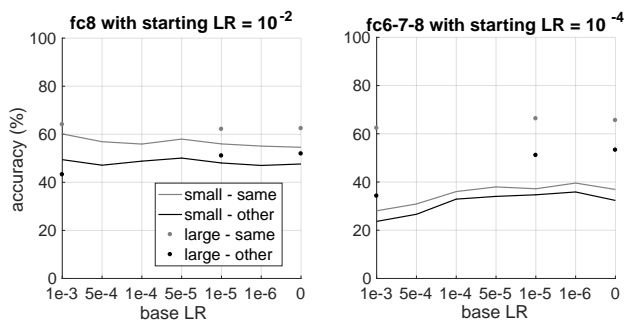


Fig. 20 Classification accuracy provided by fine-tuning *CaffeNet* according to different strategies: either learning from scratch only *fc8* (Left) or *fc6*, *fc7* and *fc8* (Right). Performance is reported for both the same day of training (Light Gray) and a different one (Dark Gray). We tried multiple values of base LR on a “small” training set (Continuous Line), and only one small, medium and large value (Dots) on a “large” one.

(Right) has much more free parameters than the one learning only the last FC layer (Left). Indeed, we notice that this latter strategy is more robust to the small-scale scenario, for any base LR (Continuous Line in the range 40-60% to the Left and 20-40% to the Right).

We also observe that, when we add frames to the training set, both strategies benefit from learning slowly (i.e., when we pass from the Continuous Line to the corresponding Dot we gain more with smaller base LR). Indeed, in the large-scale experiment learning *fc6-7-8* with small base LR achieves the best performance. On the contrary, learning only *fc8* with large base LR almost does not benefit from seeing more frames and even overfits the day of training.

Therefore, since in our analysis we aimed at spanning the size of the training set in a wide range, we chose two representative strategies providing best performance respectively in the small and large-scale experiment: learning *fc6-7-8* with small (actually 0) base LR, that we call the *conservative* strategy, to account for our larger-scale settings, and learning only *fc8* with large base LR, that we call the *adaptive* strategy, to account for smaller-scale settings.

GoogLeNet. We performed for *GoogLeNet* a similar analysis to the one reported for *CaffeNet*.

We recall that the considered *GoogLeNet* architecture is composed of “main” branch, ending with one FC layer (called *loss3/classifier*), and two identical “auxiliary” branches, ending with two FC layers (called *loss1(2)/fc* and *loss1(2)/classifier*). We refer to (Szegedy et al 2015) for a detailed description of the model. By considering this structure, we then explored the following parameters:

Base LR: varied as for *CaffeNet*.

Learned FC Layers: we always learned *loss3/classifier* from scratch with starting LR equal to 10⁻²; regarding the auxiliary branches, we tried (i) to cut them out, (ii) to learn also *loss1(2)/classifier* from scratch with starting LR equal to 10⁻², or, finally, (iii) to learn from scratch also *loss1(2)/fc*, setting the starting LR of these layers and of *loss1(2)/classifier* to 10⁻³.

Dropout %: we tried either default CAFFE values (40% for *loss3/classifier* and 70% for *loss1(2)/fc*) or a higher percentage: 60% for *loss3/classifier* and 80% for *loss1(2)/fc*.

Solver: we tried either *SGD* or *Adam* (Kingma and Ba 2015) solvers in CAFFE.

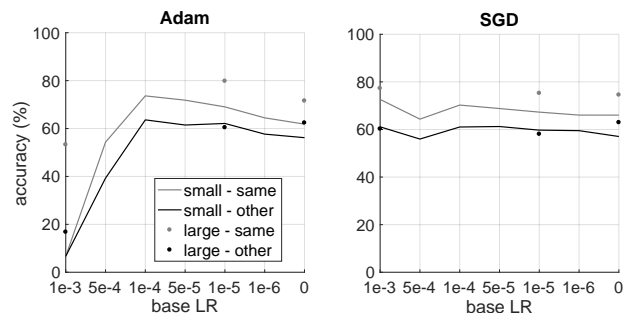


Fig. 21 Classification accuracy provided by fine-tuning *GoogLeNet* according to different strategies: either using the *Adam* solver (Left) or *SGD* (Right). The rest of the figure is similar to Fig. 20

LR Decay Policy: when using *SGD*, we used polynomial decay with exponent 0.5 or -3 ; when using *Adam*, we maintained the learning rate constant.

As for *CaffeNet*, we tried all combinations and left the not mentioned parameters to default values in CAFFE.

We first observed that, differently from *CaffeNet*, overall for this architecture the impact of learning or not the FC layers from scratch was very small, with the three tested strategies behaving very similarly. We chose the last one (iii), that was slightly better than the others. We also observed a little benefit from using higher dropout percentages.

One little more critical aspect was instead the choice of the solver. To this end, in Fig. 21 we report the accuracy obtained respectively when using the *Adam* solver (Left) or *SGD* (Right). In the latter case we applied the polynomial decay with smaller slope, since we observed again that it was consistently better. Performance is reported, as in Fig. 20, for both the same day of training (Light Gray) and a different one (Dark Gray). We varied again the base LR from 10⁻³ to 0 (horizontal axis), trying all values on the “small” experiment (Continuous Line) and one small, medium and large value for the “large” experiment (Dots).

It can be observed that, while the *SGD* solver is more robust to different choices of base LR, *Adam* provides slightly better accuracies for mid-range values of base LR, both for the small and the large experiment. We therefore opted for this latter solver.

Then, similar observations as for the *CaffeNet* architecture led us to conclude that learning slowly (with a smaller base LR) can be preferable when we add more frames to the training set, since the model is less prone to overfit the training condition (i.e. with base LR equal to 0 we gain performance on both days when passing from the Continuous Line to the corresponding Dot). Larger base LR can be preferable instead when the training set is smaller. As reported in Tab. 3 therefore, also for *GoogLeNet* we identified an *adaptive* strategy with base LR equal to 0 and a *conservative* strategy with base LR equal to 10⁻⁵.

D More Experiments on Categorization

In this section we complement the experiments discussed in the paper with further analysis. These results are reported to show that the behavior observed for the specific conditions considered in the paper (e.g. number of object classes considered for the tasks) holds also in other settings.

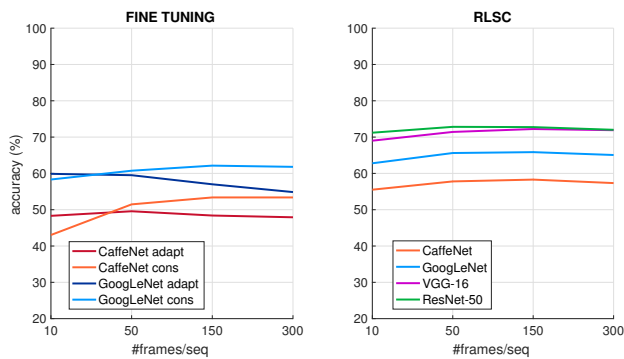


Fig. 22 Recognition accuracy vs # frames (number of object views available during training). Same experiment as Fig. 6 but executed by training only on 3 example instances per category.

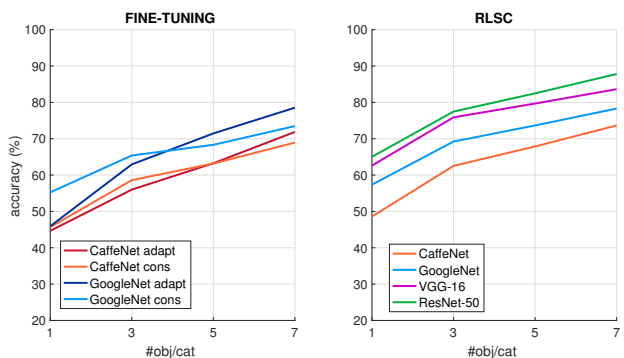


Fig. 23 Recognition accuracy vs # instances (number of object instances available during training). Same experiment as Fig. 7 executed for a 10-class categorization problem.

D.1 Increasing the Training Set Size

Fig. 22 reports the results of the same experiment shown in Fig. 6, but performed including only 3 object instances per category in the training sets. For the sake of completeness, we complement the information provided in Sec. 4.2.1 by precisizing that we considered a 15-class categorization task comprising the following categories: *cellphone, mouse, coffee mug, pencil case, perfume, remote, ring binder, soap dispenser, sunglasses, flower, wallet, glass, hairbrush, hair clip, book*.

These results further confirm that, in this setting, adding frames without increasing semantic variability cannot be used as a viable strategy to improve categorization accuracy, that remains definitely lower than the performance achieved using 7 example instances (Fig. 6).

D.2 Increasing the Semantic Variability

Fig. 23 and 24 report the results of an experiment analogous to the one shown in Fig. 7, but for respectively 10 and 5 object categories rather than 15. As can be noticed, the observations reported in Sec. 4.2.2 apply also here, namely the accuracy increases remarkably as more example instances per category are made available (without saturating), supporting the claim that semantic variability is indeed critical for categorization even in settings that involve few categories.

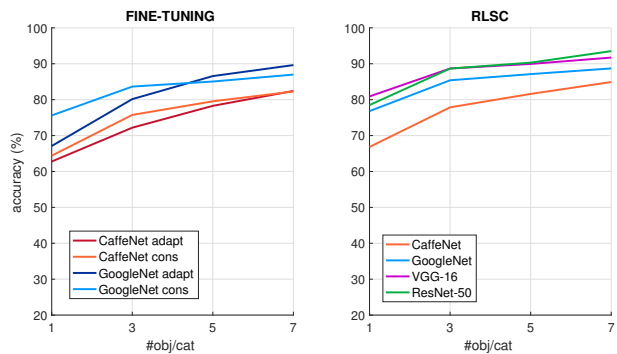


Fig. 24 Recognition accuracy vs # instances (number of object instances available during training). Same experiment as Fig. 7 executed for a 5-class categorization problem.

D.3 Improving Invariance of CNNs on Categorization

As mentioned at the end of Sec. 5.2.1, here we verify whether the approach adopted to improve the invariance of CNNs in identification settings may also be adopted to improve performance for categorization.

We considered the 15-class categorization task of Sec. 4.3, Fig. 9, performed by sampling ~ 20 frames per sequence and applying RLSC on top of representations extracted by off-the-shelf CNNs. In this experiment we compared the performance on this task achieved by applying RLSC on top of representations extracted by CNNs which had been previously fine-tuned. To this end, as in Sec. 5.2.1, we evaluated the impact of different fine-tuning strategies.

Specifically, we considered exactly the same fine-tuned models as in Sec 5.2.1 for the first three strategies (namely, **iCWT id**, **iCWT cat**, **iCWT + ImNet**) and, for the last one (**ImNet**), we fine-tuned over the 15 ImageNet synsets corresponding to the 15 categories that will be later involved in the categorization task. We report results in Fig. 25 using the same notation as in Fig. 12: as anticipated, none of these strategies is beneficial when considering a categorization task. Indeed, we do not achieve any improvement in performance with respect to the off-the-shelf baseline.

E Generalization Across Days

In this section we test the robustness of the considered visual recognition systems with respect to variations such as changes of illumination, background, etc., which are neither semantic nor geometric. In the current release of iCWT, for each object instance we have acquired image sequences in two different days, in order to naturally have images with these kind of variations. For the sake of brevity, in the main paper we did not report on experiments related to this aspect, which is however relevant.

When training for visual recognition on a given day and testing on a second one, the possibly small contextual variation in the scene can cause the system to experience a degradation of its recognition accuracy. In the experiments reported below, we report this loss as the difference between the average classification accuracy observed when testing a model on the same day it was trained on and on the other available day in iCWT.

In particular, we consider the models trained for the categorization experiment in Sec. 4.2.1 and Sec. 4.2.2, and for

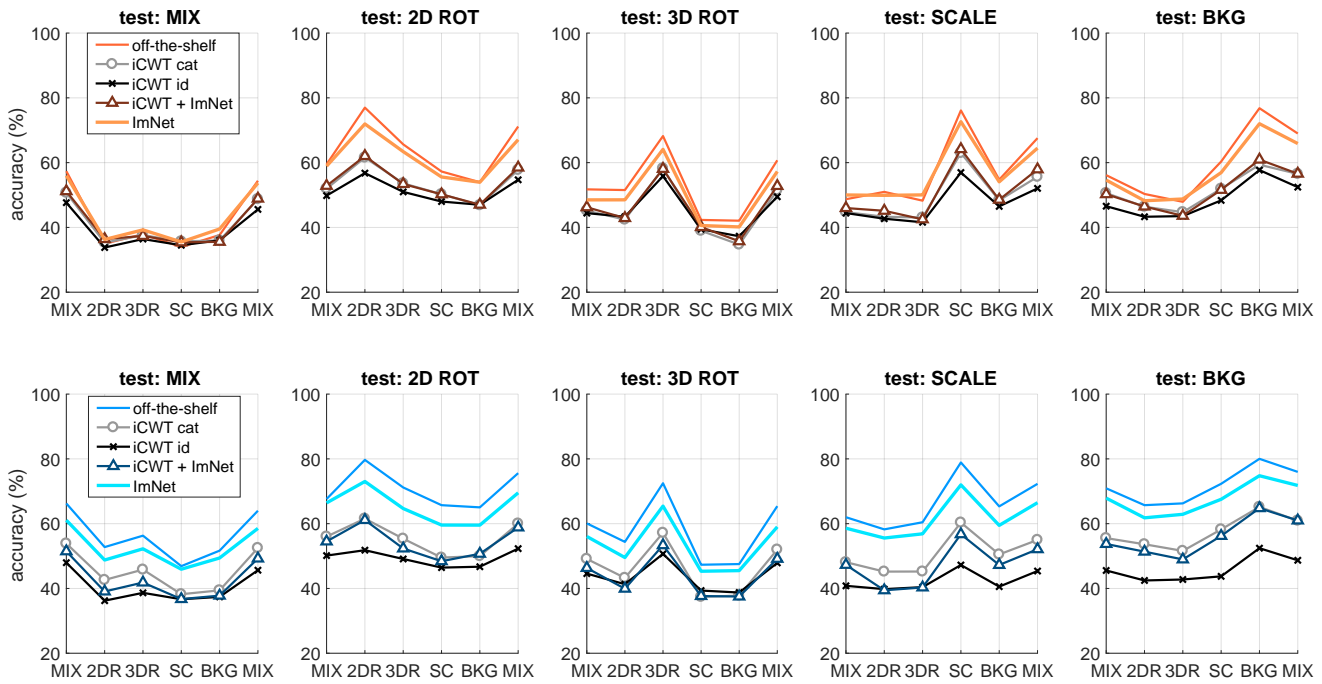


Fig. 25 Same experimental setting as in Fig. 9, but using different image representations, provided by CaffeNet (Top, Orange) or GoogLeNet (Bottom, Blue), network models fine-tuned according to different strategies (see Sec. D.3).

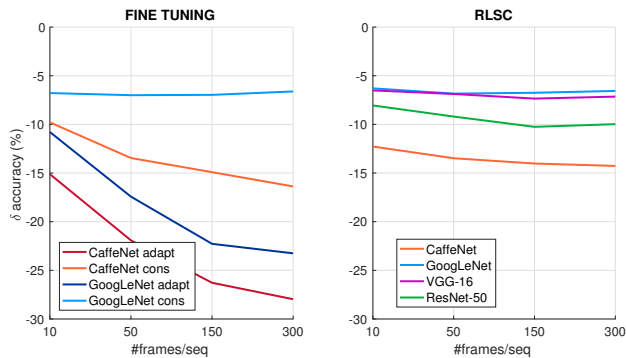


Fig. 26 Categorization accuracy vs # frames - Generalization across days. Drop in performance (difference between test accuracy) observed when testing the models trained for the categorization task reported in Sec. 4.2.1 on the same day of training and on a different one.

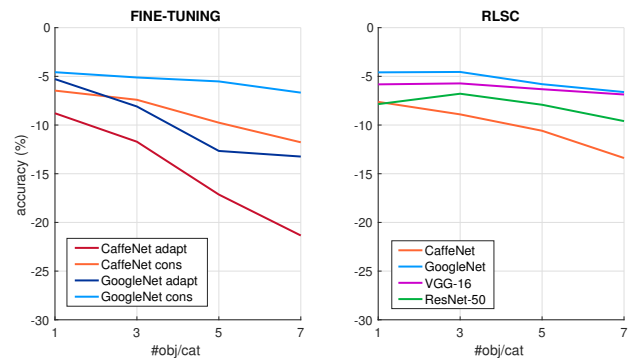


Fig. 27 Categorization accuracy vs # instances - Generalization across days. Drop in performance (difference between test accuracy) observed when testing the models trained for the categorization task reported in Sec. 4.2.2 on the same day of training and on a different one.

identification in Sec. 5.1. In this section, we test these models on a day different from the one used for training (that is, we took the images of the object instances selected for testing in the original experiment, but from the second available day).

Categorization Fig. 26 and Fig. 27 report the loss in performance observed in the categorization setting, respectively for the case where we tested on the relevance of the training set size (see Fig. 6) and of semantic variability (see Fig. 7). Surprisingly, in both settings all networks exhibit a substantial drop in performance, of the order of more than 5% accuracy and in some cases even around 20%. Critically, the *adaptive* fine-tuning strategy, which appeared more effective when tested on the same day, is also the strategy that leads to the biggest drop. This implies that the CNN is overfitting

the variability the training day and is therefore less capable of generalizing to other days. Interestingly however, when using less aggressive strategies such as the *conservative* fine-tuning or the feature extraction based classifier, modern networks such as *GoogLeNet* and *ResNet-50* seem in general quite robust.

Identification The dramatic loss in performance observed for the *adaptive* fine-tuning in categorization could be in principle worrisome if we recall that, in the *identification* setting, such strategy was adopted in Sec. 5.2.1 to improve the invariance properties of CNNs on a preliminary dataset. Interestingly however, in Fig. 28 we notice that, in the identification setting, the *adaptive* fine-tuning strategy seems to be not

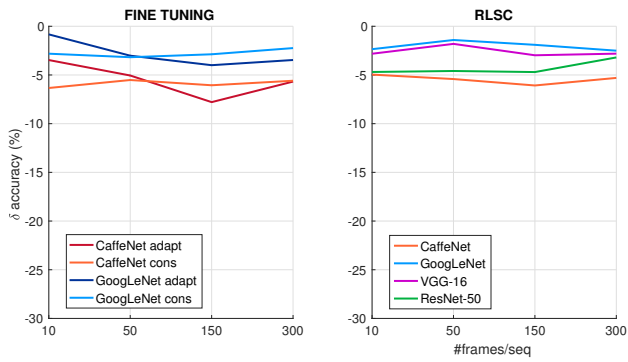


Fig. 28 Identification accuracy vs # frames - Generalization across days. Drop in performance (difference between test accuracy) observed when testing the models trained for the identification task reported in Sec. 5.1 on the same day of training and on a different one.

overfitting the training day and, albeit experiencing a drop in performance when generalizing to another day, such loss is small and on par with the other strategies considered in this work. Indeed, it can be noticed that all methods exhibit a performance drop around $\sim 5\%$ in accuracy.